# EMERGING HUMAN PROTOPARVOVIRUSES

## - IN SEARCH OF ACUTE INFECTIONS

MAIJA JOKINEN

MASTER'S THESIS

UNIVERSITY OF HELSINKI
FACULTY OF BIOLOGICAL AND ENVIRONMENTAL SCIENCES
GENERAL MICROBIOLOGY

SPRING 2019

| Tiedekunta – Fakultet – Faculty | Koulutusohjelma – Utbildingsprogram – Degree Programme |
|---|---|
| Faculty of Biological and Environmental Sciences | Degree Programme in Molecular Biosciences |

Tekijä – Författare – Author
Maija Jokinen

Työn nimi – Arbetets titel – Title
Emerging human protoparvoviruses –in search of acute infections

Oppiaine/Opintosuunta – Läroämne/Studieinriktning – Subject/Study track
General microbiology

| Työn laji – Arbetets art – Level | Aika – Datum – Month and year | Sivumäärä – Sidoantal – Number of pages |
|---|---|---|
| Master's thesis | February 2019 | 54 |

Tiivistelmä – Referat – Abstract

Parvoviruses are among the smallest known viruses. The parvovirus genome is a single stranded DNA, approximately 5 kb in size. The virion has a small (20 to 30 nm), rugged, non-enveloped icosahedral capsid. Parvoviruses can cause a number of diseases. Possibly the most recognized human parvovirus is parvovirus B19 (B19V), which can cause the so-called fifth disease, anemias and fetal death. Another relatively well characterised parvovirus is human bocavirus 1 (HBoV1), which causes respiratory tract infections in young children.

Bufavirus (BuV) tusavirus (TuV) and cutavirus (CuV) are emerging parvoviruses, discovered during the years 2012-2016 using next generation sequencing methods. All three viruses were originally discovered in feces of patients suffering from diarrhea. BuV was originally found in Burkina Faso and has since been detected in fecal samples with polymerase chain reaction (PCR)-based methods from Europe, Asia and Africa. The seroprevalence of BuV differs between countries. TuV was found in a single stool sample from Tunisia, but no further reports of it have since emerged. CuV was found in 2016 and it has been linked to cutaneous T-cell lymphoma, but it is not known if the virus is the cause of the cancer or if the virus simply prefers quickly dividing cancer cells for its replication. BuV, TuV and CuV belong to the *Protoparvovirus* genus, but it is still unclear whether TuV is a human pathogen. More research is needed to study the epidemiology of these viruses and their role in illnesses.

There were two main aims in this thesis: to set up an IgM µ-capture enzyme immunoassay (EIA) for human protoparvoviruses using BuV1 as an example and to screen three stool sample cohorts for BuV, TuV and CuV using an in-house multiplex quantitative PCR (qPCR). The IgM EIAs developed for B19V and HBoV1 was used as the base for developing human protoparvovirus IgM EIA, using Virus-like particles (VLP) as antigens. Setting up the EIA required a great amount of optimization and finally troubleshooting, since the assay did not work as expected. The troubleshooting revealed that the ambiguous results in the IgM µ-capture EIA were possibly due to degraded VLPs or that the sensitive µ-capture format requires extremely carefully purified VLPs. More optimizing is needed for this assay, however, the work done in this thesis offers a good base for further development of protoparvovirus IgM EIA. All three viruses were found in the stool samples during multiplex qPCR screening. Based on the qPCR and sequencing results one sample was positive for BuV DNA, one sample for TuV DNA and a total of 12 samples for CuV DNA. This is the first time TuV DNA has been found since its discovery. In addition to that, CuV DNA was identified in fecal samples for the first time since the discovery, previously CuV DNA had been found mostly in skin biopsies. As for TuV, based on the parvovirus phylogenetic analyses, its sequence is more closely related to rodent parvoviruses than CuV or BuV. More research is needed, possibly with animal and human samples, to establish the role of TuV as a human virus.

Avainsanat – Nyckelord – Keywords
Parvovirus, qPCR, EIA, IgM, DNA viruses, emerging viruses

Ohjaaja tai ohjaajat – Handledare – Supervisor or supervisors
Ausra Domanska, Maria Söderlund-Venermo

Säilytyspaikka – Förvaringställe – Where deposited
E-thesis

Muita tietoja – Övriga uppgifter – Additional information

| Tiedekunta – Fakultet – Faculty | Koulutusohjelma – Utbildingsprogram – Degree Programme |
|---|---|
| Bio- ja ympäristötieteellinen tiedekunta | Molekyylibiotieteiden koulutusohjelma |

Tekijä – Författare – Author
Maija Jokinen

Työn nimi – Arbetets titel – Title
Emerging human protoparvoviruses- in search of acute infections

Oppiaine/Opintosuunta – Läroämne/Studieinriktning – Subject/Study track
Yleinen mikrobiologia

| Työn laji – Arbetets art – Level | Aika – Datum – Month and year | Sivumäärä – Sidoantal – Number of pages |
|---|---|---|
| Pro gradu | Helmikuu 2019 | 54 |

Tiivistelmä – Referat – Abstract
Parvovirukset ovat eräitä pienimpiä tunnettuja viruksia. Parvovirusten genomi on yksijuosteinen DNA, jonka koko on noin viisituhatta emäsparia. Parvovirus virionilla on pieni (20-30 nm), vaipaton ikosahedraalinen kapsidi. Parvovirukset voivat aiheuttaa monenlaisia infektioita. Kenties tunnetuin ihmiselle patogeeninen parvovirus on parvovirus B19 (B19V), joka aiheuttaa parvorokkoa, anemioita ja sikiökuolemia. Toinen paljon tutkittu parvovirus on ihmisen bocavirus 1 (HBoV), joka aiheuttaa pienten lasten hengitystieinfektioita.

Bufavirus (BuV), tusavirus (TuV) ja cutavirus (CuV) ovat uusia parvoviruksia, jotka löydettiin vuosina 2012–2016 syväsekvensointimenetelmillä. BuV löydettiin alun perin ulostenäytteestä Burkina Fasosta ja virusta on sen jälkeen löydetty polymeraasiketjureaktioon (PCR) perustuvien menetelmien avulla ulostenäytteistä Euroopasta, Afrikasta ja Aasiasta. BuV:n seroprevalenssi vaihtelee alueittain. TuV löydettiin yhdestä ainoasta ulostenäytteestä Tunisiasta, eikä TuV DNA:ta ole löydetty sen jälkeen muista näytteistä. CuV löydettiin vuonna 2016 ja se on yhdistetty kutaaniseen T-solulymfoomaan, mutta ei tiedetä aiheuttaako virus syövän vai hakeutuuko se vain nopeasti jakautuviin syöpäsoluihin. BuV, TuV ja CuV kuuluvat *Protoparvovirus* sukuun, mutta ei tiedetä onko TuV ihmisen virus. Kaikkien kolmen uuden parvoviruksen tutkimus on vielä alussa. On paljon, mitä ei tiedetä näiden kolmen viruksen epidemiologiasta ja niiden aiheuttamista oireista.

Tämän pro gradu – työn kahtena päätavoitteena oli: pystyttää µ-kaappaus-IgM-entsyymivälitteinen immunosorbenttimääritys (EIA) -testi ihmisen protoparvoviruksille käyttäen BuV1:ta esimerkkinä sekä analysoida kolme ulostenäytekohorttia valmiilla BuV, TuV ja CuV kvantitatiivisella multiplex PCR (qPCR)-menetelmällä. IgM EIA:n pystytyksen perustana käytettiin aiemmin HBoV:lle ja parvovirus B19V:lle pystytettyjä µ-kaappaus-IgM-EIA-testejä. Menetelmää jouduttiin optimoimaan paljon ja lopulta monia testauksia jouduttiin tekemään, sillä menetelmä ei toiminut kuten oli oletettu. Vian etsinnän tuloksena saatiin selville, että epäselvät tulokset saattoi aiheuttaa hajonneet VLP:t tai, että herkkä µ-kaappaus-testi vaatii erityisen puhtaita VLP:tä. Lopullista toimivaa µ-kaappaus-IgM-EIA-menetelmää protoparvoviruksille ei tässä työssä pystytty pystyttämään, mutta tämä työ luo hyvän pohjan jatkokehitykselle. BuV, TuV ja CuV DNA:ta löydettiin ulostenäytteistä multiplex qPCR-menetelmällä. QPCR- ja sekvensointitulosten perusteella tässä työssä löydettiin yksi BuV DNA-positiivinen ja yksi TuV DNA positiivinen näyte. Lisäksi löydettiin 12 CuV DNA positiivista näytettä. TuV DNA:ta havaittiin ensi kertaa sen ensilöydön jälkeen. Sen lisäksi, CuV DNA:ta löydettiin ensilöydön jälkeen jälleen ulostenäytteestä. Useissa aiemmissa tutkimuksissa CuV DNA:ta on löydetty ihosta otetuista biopsioista. Fylogeneettisten analyysien perusteella TuV:n sekvenssi on lähempänä jyrsijöiden parvoviruksia kuin BuV:n ja CuV:n sekvenssit. Tutkimusta ja erilaisia näytteitä (eläin- ja ihmisperäisiä) tarvitaan, jotta voidaan selvittää onko TuV ihmisen virus.

Avainsanat – Nyckelord – Keywords
Parvovirus, qPCR, EIA, IgM, DNA-virukset, uudet parvovirukset

Ohjaaja tai ohjaajat – Handledare – Supervisor or supervisors
Ausra Domanska, Maria Söderlund-Venermo

Säilytyspaikka – Förvaringställe – Where deposited
E-thesis

Muita tietoja – Övriga uppgifter – Additional information

*Usko minua; mikään ei ole niin vaarallista kuin sisällä istuminen. Silloin saa helposti kaikenlaisia aatteita, selitti Hemuli.*

Hemuli, Taikatalvi

# CONTENTS

LIST OF ABBREVIATIONS

| | |
|---|---|
| AAV | Adeno-Associated Virus |
| BLAST | Basic Local Alignment Search Tool |
| BSA | Bovine Serum Albumin |
| BuV | Bufavirus |
| Cq | Quantification Cycle |
| CTCL | Cutaneous T-Cell Lymphoma |
| CuV | Cutavirus |
| DNA | Deoxyribonucleic Acid |
| dsDNA | Double-stranded DNA |
| EDTA | Ethylenediaminetetraacetic Acid |
| EIA | Enzyme Immunoassay |
| ELISA | Enzyme-Linked Immunosorbent Assay |
| HBoV | Human Bocavirus |
| HRP | Horseradish Peroxidase |
| ICTV | International Committee on Taxonomy of Viruses |
| IgM | Immunoglobin M |
| IgG | Immunoglobin G |
| kb | Kilobase |
| kDa | Kilodalton |
| LOD | Limit of Detection |
| nm | Nanometer |
| NS | Non-Stuctural |
| qPCR | Quantitative Polymerase Chain Reaction |
| PCR | Polymerase Chain Reaction |
| MVM | Minute Virus of Mice |
| NS | Non-structural protein |

| | |
|---|---|
| PBS | Phosphate Buffered Saline solution |
| PBST | Phosphate Buffered Saline solution with 0.05 % of Tween 20 |
| PARV4 | Parvovirus 4 |
| RPM | Rounds Per Minute |
| ssDNA | Single-Stranded DNA |
| TE | Tris-EDTA buffer |
| TuV | Tusavirus |
| VLP | Virus-Like Particle |
| VP | Viral (structural) Protein |

# 1. INTRODUCTION

Well over 200 viruses are known to be pathogenic to humans (Bibby, 2013). New viruses have traditionally been identified based on the patient symptoms combined with methods such as: viral culture, electron microscopy, serology, cytology and histology. These techniques are effective but have certain limitations. For example, not all viruses can be cultured in laboratory conditions and some of the traditional techniques can be time consuming (Storch, 2007). Rapid developments in the fields of sequencing, bioinformatics and metagenomics have revolutionized the discovery of novel human viruses. With the high-throughput sequencing methods it is possible to gain extensive amounts of sequence data, simultaneously. Viral metagenomics is a technique where the whole viral nucleotide sequence content (virome) (Bexfield & Kellam, 2011) of an uncultivated sample, e.g. from marine environments (Breitbart *et al.*, 2002) or human blood (Jones *et al.*, 2005), can be sequenced and analyzed.

Due to high-throughput sequencing and metagenomics, several putative human pathogens have been found in the last fifteen years: Karolinska Institutet (KI) polyomavirus, human bocavirus 1 (HBoV1), astrovirus VA1, Washington University (WU) polyomavirus, Lujo virus, trichodysplasia spinulosa polyomavirus and human parvovirus (PARV4) (Allander *et al.*, 2007; Allander *et al.*, 2005; Finkbeiner *et al.*, 2009; Gaynor *et al.*, 2007; Briese *et al*., 2009; Janssens *et al.*, 2010; Jones *et al*., 2005). Among the newly discovered viruses are also members of the parvovirus family. Bufavirus (BuV), Tusavirus (TuV) and cutavirus (CuV), have been identified in recent years during viral metagenomic studies (Phan *et al*., 2014; Phan *et al.*, 2012; Phan *et al.*, 2016). The clinical significance of TuV, BuV and CuV is yet to be unraveled and more research is needed to clarify their pathogenicity. With new viruses being discovered at a faster rate than before, the need for assessing their clinical significance and the need for rapid diagnostics will become even more important (Tang & Chiu, 2010). In the following chapters I will describe the family *Parvoviridae* and BuV, TuV and CuV in more detail. I will also describe the theory behind the main methods used in this work.

### 1.1. Family *Parvoviridae*

Parvoviruses are among the smallest known viruses when it comes to the size of the virion and the size of the genome. The size of the virion is approximately 25 nanometers (nm) in diameter (Berns & Parrish, 2013) and the genome is a linear single-stranded DNA (ssDNA) with an average size around 5 kilobases (kb) (Cotmore & Tattersall, 2014). Despite the small size of the genome and the particle itself, parvoviruses are a diverse group of viruses able to infect hosts from cats to humans to cockroaches (Bowles *et al.*, 2006; Mukha *et al.*, 2006; Cotmore *et al.*, 2019). The family *Parvoviridae* is divided into two subfamilies based on the host: viruses that belong to *Densovirinae* infect invertebrates and viruses from *Parvovirinae* infect vertebrates (Cotmore *et al.*, 2014). Based on the sequence and phylogenetic analyses, five parvovirus genera are grouped into *Densovirinae* subfamily and eight genera into *Parvovirinae* subfamily (Figure 1) (Cotmore *et al.*, 2019; Cotmore & Tattersall, 2007). As of October 2018, there were 58 International Committee on Taxonomy of Viruses (ICTV) approved species in the *Parvovirinae* subfamily.

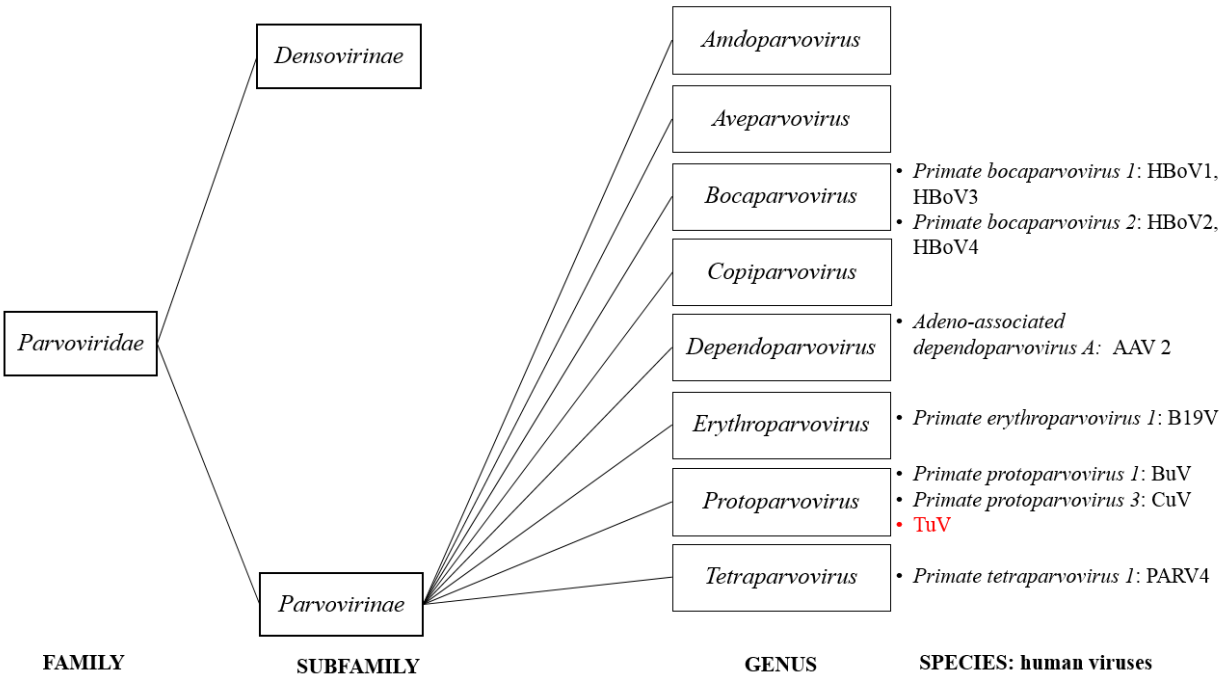


**Figure 1**. Taxonomy of the *Parvoviridae* family, subfamilies *Densovirinae* and *Parvovirinae* and all the *Parvovirinae* genera with a few example species. Tusavirus (marked in red) is still an unclassified member of genus *Protoparvovirus* (Cotmore *et al.*, 2019).

The parvovirus capsids are rugged, non-enveloped icosahedrons with T=1 symmetry, consisting of 60 copies of 1-3 structural proteins (VP1-VP3) (Berns & Parrish, 2013). The ~5 kb genome usually

consists of two major genes, non-structural (*NS*) and structural (*VP*), which are regulated by one or more promoters (Figure 2), depending on the virus. The *NS* gene encodes a multipurpose protein NS1, which regulates the viral cycle on different levels. NS1 is essential in regulation of viral gene expression through activation of parvovirus promoters, DNA replication (Zhi *et al.*, 2006), and transactivation of host genes (Lou *et al.*, 2012). NS1 has DNA-binding and nicking domains (Op De Beeck & Caillet-Fauquet, 1997) and cytotoxic properties (Hristov *et al.*, 2010) inducing apoptosis (Moffat *et al*., 1998). The *VP* gene encodes one long capsid protein (VP1) and different length variants by alternative splicing (VP2-VP5), depending on the virus (Cotmore & Tattersall, 2014; Qiu *et al.*, 2017). BuV, TuV and CuV genomes encode two major genes: *NS* and *VP*. The two genes translate to three major proteins NS1, VP1 and VP2, of which VP1 and VP2 by alternative splicing (Väisänen *et al.*, 2017, Altay *et al.*, 2015, Phan *et al*., 2014).

The parvovirus ssDNA strand is distinctively flanked by two short imperfect palindromic sequences. The flanking sequences can fold back in both termini of the DNA sequence creating terminal loops or hairpins (Figure 2) and play a great role in parvovirus replication. Parvoviruses replicate using a unique mechanism called “rolling hairpin”, described already in 1976 (Tattersall & Ward, 1976). The rolling hairpin is an adaptation of the rolling-circle replication system ( Li, 2013) used by bacteria for plasmid replication and by many circular dsDNA (double-stranded DNA) viruses for genome replication (Ruiz-Maso *et al.*, 2015). The hairpins act as primers for the complementary strand during replication (Berns & Parrish 2013). The synthesis of the complementary strand is dependent on host polymerases and the elongation is followed by complicated series of folding back and forth before the new DNA strand is ready (Cotmore and Tattersall, 2014).

The hairpin structures are diverse among members of *Parvoviridae* and can differ in size, sequence and structure (Deiss *et al.*, 1990; Li, 2013). For example, HBoV1 and parvovirus B19 (B19V) have hetero- and homotelomeric hairpin structures, respectively (Astell *et al.*, 1989; Huang *et al.*, 2012; Luo & Qiu, 2015). The hairpin structures for BuV, TuV and CuV are unknown, but are thought to be similar to other protoparvoviruses e.g. minute virus of mice (MVM) (Figure 2) (Väisänen *et al.*, 2017).

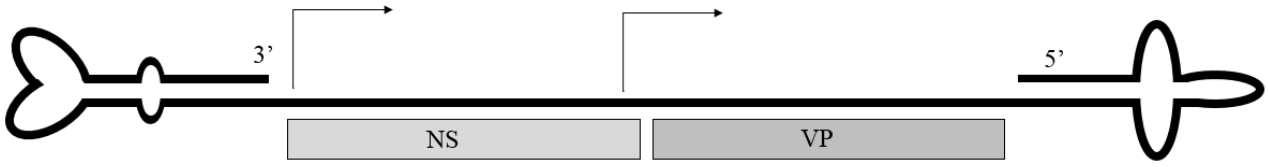


**Figure 2.** A simplified illustration of a typical parvovirus (minute virus of mice) genome organization showing the terminal hairpin structures and the two promoters, indicated by two curved arrows. The left side encodes the non-structural (NS) region and the right side for structural (VP) region (Cotmore and Tattersall, 1986; Cotmore *et al.*, 2019).

Parvoviruses are transmitted through various routes: via the respiratory route (B19V and HBoV1) (Qiu *et al.*, 2017), via intrauterine transmission and blood-products (B19V) (Brown, 2006), via the fecal-oral route (canine parvovirus and feline parvovirus) (Parrish & Hueffer, 2006). Parvoviruses lack proteins capable of inducing resting cells to enter an interphase. Infections are limited to dividing cells (Cotmore and Tattersall, 2013), except for HBoV1 which can replicate in non-dividing human epithelial cells with the help of the cellular DNA damage response and repair system (Deng *et al*., 2016; Huang *et al*., 2012). Parvoviruses enter the host cell by binding to specific cell surface receptors and by receptor mediated endocytosis (Vihinen-Ranta *et al.*, 2002; Vihinen-Ranta & Parrish, 2006). When entering the cell, the virion undergoes conformational changes which result in exposure of a phospholipase $A_2$ ($PLA_2$) motif in VP1 (Bleker *et al.*, 2005; Farr *et al.*, 2005) at the capsid surface (Vihinen-Ranta *et al.*, 2002).

Not a lot is known of parvovirus intracellular traffiking, but it is suggested that $PLA_2$ activity is utilized during intracellular traffiking and is resposible for damaging the late endosome prior to nuclear entry (Farr *et al.*, 2005, Zadori *et al.*, 2001). After nuclear entry parvoviruses hi-jack the host replication system. How parvoviruses utilize the host replication system, is not fully understood. A recent study shows that B19V can alter the cell signalling pathways and induce cell cycle arrest resulting in a prolonged S-phase (Zou *et al.*, 2017). During the prolonged S-phase the virus can utilize the host replication system for viral replication. The produced mRNA is translated on cellular ribosomes in the cytoplasm and the structural proteins are transported back to the nucleus as trimers (Lombardo *et al.*, 2002), where the virions are assembled and new genomes are encapsidated. The virions are released by inducing apoptosis at the end of the infection (Moffatt *et al.*, 1998; Schmidt *et al.*, 2002). Release of progeny virus prior to apoptosis has been described for MVM and HBoV1 (Deng *et al.*, 2013; Maroto *et al.*, 2004). The rapid export pathway utilizes the nuclear export protein CRM1 and transport through the Golgi (Bär *et al*., 2013).

### *1.1.1. A short history of parvoviruses*

The first discovered parvovirus (lat. *parvus* = small) was the Kilham rat virus (KRV) in 1959 isolated from a rat tumor (Kilham & Olivier, 1959). KRV has been extensively studied and it is now known that the virus is widely spread in rodents and can cause fetal death or trigger autoimmune diabetes in rats (Chung *et al.*, 2014; Ellerman *et al.*, 1996). Atchinson *et al.* (1965) found small virus-like particles from rhesus monkey kidney cell cultures infected with simian adenovirus type 15, they referred to the newly found particle as adenovirus associated virus (AAV). AAV was later identified as parvovirus and further studies have shown that AAV can infect humans but is non-pathogenic (Qiu *et al.*, 2017). These qualities make AAV a very interesting candidate for gene therapy. AAV is intensively studied as a viral vector and some clinical trials of using AAV in gene therapy are already taking place (Rangarajan *et al.*, 2017).

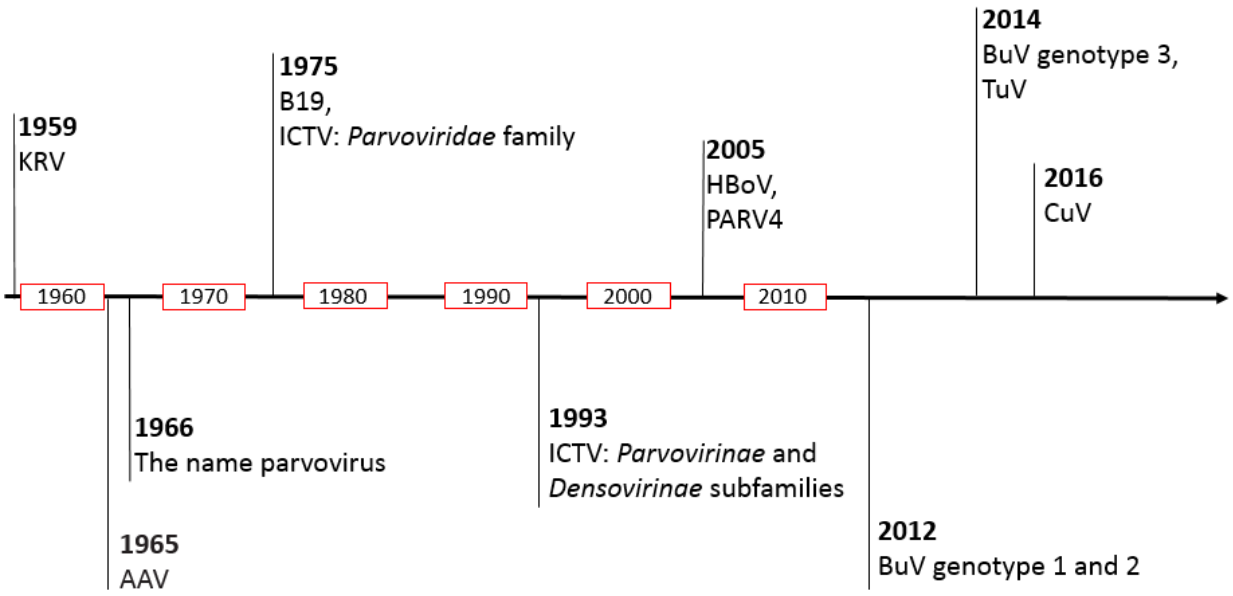


**Figure 3.** Parvovirus timeline from the discovery of KRV, the founding member of the *Parvoviridae* family, to the year 2016, when CuV, an emerging human protoparvovirus, was discovered.

B19V was found in 1975 (Cossart *et al.*,1975) in human sera. B19V infections are very common especially among children and appear as a rash also called fifth disease (*erythema infectiosum*) (Anderson *et al.*,1983). Maternal B19V infection can cause fetal death, if the infection is acquired during the first months of pregnancy (Brown *et al.*, 1984). In 1975 the *Parvoviridae* family was officially accepted by ICTV (ICTV, 1975). Three decades passed until a new human pathogenic

parvovirus was found (Figure 3). Human bocavirus 1 (HBoV1) and PARV4 were both identified in 2005 (Allander *et al.*, 2005; Jones *et al.*, 2005) in viral metagenomics studies. HBoV1 was found in respiratory tract samples of a young child with symptomatic respiratory tract infection. After 2005, three additional human bocaviruses (HBoV2-4) were discovered, all in diarrheic stool samples (Kapoor *et al.*, 2009, Arthur *et al.*, 2009; Kapoor *et al.*, 2010). HBoV1 is strongly linked to respiratory tract infections, especially among young children (Allander *et al.*,2007; Maggi *et al.*, 2007; Zheng *et al.*, 2010), whereas for HBoV2-4, the clinical pictures are unclear. HBoV2-4 are mainly detected from stool samples (Santos *et al.*, 2010, Kantola *et al.*,2011) and there is some evidence linking these viruses to gastrointestinal infections (Arthur *et al.*, 2009). PARV4 was first identified in a plasma sample of intravenous drug user, with symptoms of acute viral syndrome (Jones *et al.*,2005). PARV4 infection is strongly associated with other viral infections, such as human immunodeficiency virus, hepatitis C or hepatitis B (Matthews *et al.*, 2014). The clinical significance and definitive symptoms of PARV4 are still unclear (Sharp *et al.*, 2010). After 2010, three novel putative human pathogenic parvoviruses have been discovered: BuV, CuV and TuV (Phan *et al.*, 2014; Phan *et al.*, 2012; Phan *et al.*, 2016).

## 1.2. Emerging human protoparvovirus*es*

### *1.2.1. Bufavirus is the most reported new Protoparvovirus*

During a metagenomics project in 2012, a virus resembling parvovirus was found in a fecal sample collected from a child suffering from acute diarrhea in Burkina Faso (Phan *et al.*, 2012). This newly found virus shared an amino-acid sequence identity of <39% in NS1 and <31% in VP1 with known parvoviruses. The parvovirus-like sequence was detected by PCR in 4% of the analysed samples (4/98) (Phan *et al.*, 2012). One of the discovered viruses shared only >73% amino acid identity in the VP2 with the other three virus sequences, indicating it was a different genotype. The viruses were named bufavirus 1 (BuV1) and bufavirus 2 (BuV2) and listed in GenBank with accession numbers JQ918261 and JX027297, respectively. Bufavirus 3 (BuV3) was initially identified in 2014 in Bhutan (Yahiro *et al.*, 2014). The virus was found in 0.8 % (n=393) of stool samples collected from children with diarrhea (age >5 years). No other virus known to cause diarrhea was discovered in the BuV-positive samples (Yahiro *et al.*, 2014). According to ICTV parvoviruses in the same species must share over 85 % of amino acid identity in the NS1 (Cotmore *et al.*, 2014). Phylogenetic analyses show that all three BuV genotypes share high amino acid sequence identities in the NS1 protein (Figure 4) and can consequently be classified in one species: *Primate protoparvovirus 1*.

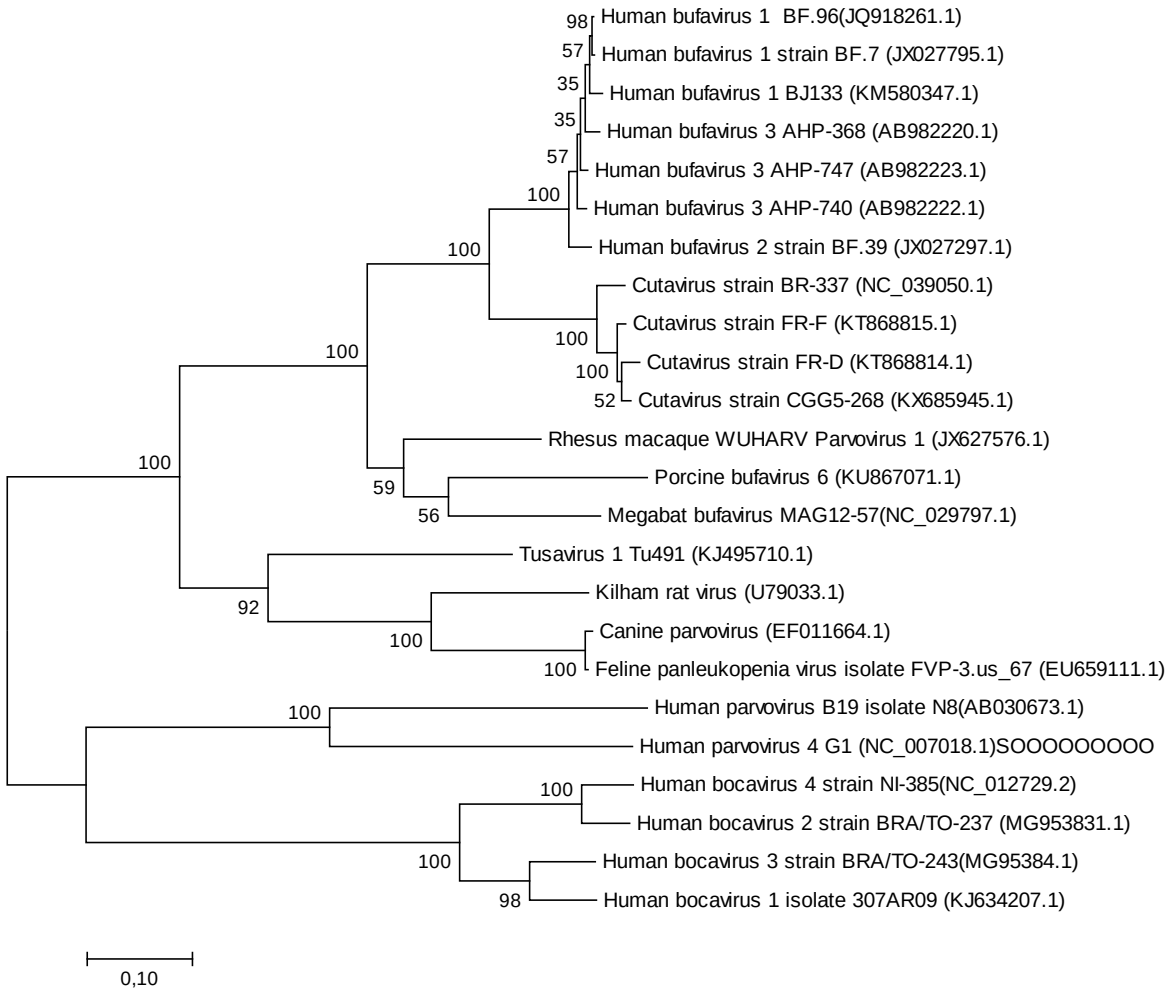


**Figure 4.** Molecular phylogenetic analysis of a group of parvoviruses by the maximum likelihood method based on the virus *NS1* gene nucleotide sequence. For the phylogenetic analyses traditional examples of parvoviruses were chosen as well as strains of emerging parvoviruses that had, if possible, full-length sequences of NS1 and VP1 regions available in GenBank (https://www.ncbi.nlm.nih.gov/genbank/). The maximum likelihood method is based on the Tamura-Nei model (Tamura & Nei, 1993). The tree was generated with 1000 bootstraps and is drawn to scale, with branch lengths measured in the number of nucleotide substitutions per site. The percentage in which the taxa is clustered is shown next to the branches. The nucleotide sequences were aligned with ClustalW with open gap penalty of 10 and gap extension penalty of 0.1. Evolutionary analyses were conducted in MEGA7 (Kumar *et al.*,2016).

Since the first discovery in 2012, BuV DNA has been detected by PCR primarily in fecal samples in Finland, the Netherlands, Thailand, Tunisia, Turkey and also in one nasal swab sample in Finland (Väisänen *et al.*, 2014; 2018, Chieochansin *et al.*, 2015, Smits *et al.*, 2014, Altay *et al.*, 2015). These findings suggest that the virus is widely spread. Enzyme immunoassay (EIA) has been developed for all three BuVs (Väisänen *et al.*, 2016). Väisänen et al. (2018) discovered that the BuV immunoglobulin G (IgG) antibody seroprevalence is significantly high in adults in Iran (56.1 %), Iraq

(84.8 %) and Kenya (72.3 %), while the seroprevalence is very low in Finland (1.9 %) and in the United States (3.6 %). This suggests that there are considerable differences in BuV distribution on a global level.

### *1.2.2. Cutavirus is linked to cutaneous T-cell lymphoma*

Cutavirus was first discovered in 2016 during another metagenomics study (Phan *et al.*,2016). Two nearly full-length viral sequences resembling the BuV sequence were obtained from stool samples of two (n=245) Brazilian children suffering from diarrhea (CutaV-BR-337 and -450, GenBank accession no. KT868811 and KT868812, respectively). The group compared the gained sequences to existing metagenomic data and found corresponding sequences from skin biopsies of two patients with cutaneous T-cell lymphoma (CTCL), suggesting a possible connection to cancer. Results were confirmed with PCR and by sequencing (Phan *et al.*, 2016). Based on sequence analysis, the discovered CuVs shared amino-acid identities of 76% and 82% in the NS1 and VP1 proteins, respectively, with BuV2 (Phan *et al.*, 2016).

In the past few years CuV has been detected mainly using PCR-based methods. CuV DNA was detected in a cutaneous malignant melanoma lesion sample in Denmark (CutaV CGG5–268, GenBank accession no. KX685945) (Mollerup *et al.*,2017) and in 6/189 (3.2%) paraffin-embedded skin biopsy samples of CTCL patients (Kreuter *et al.*, 2018) by PCR. Kreuter et al. (2018) did not observe CuV DNA in skin samples of patients with other forms of lymphomas. Väisänen *et al*. (2018) detected CuV DNA by PCR in 4/25 (16%) and in 4/136 (2.9%) skin biopsies of CTCL patients and organ transplant patients, respectively, whereas 159 healthy skin samples from 98 immunocompetent healthy individuals were CuV-DNA negative. Furthermore, Väisänen *et al.* found CuV IgG antibodies in serum samples of the same groups: CTLC patients (9.5%), organ transplant patients (6.5%) and in healthy adults (3.8%). Based on these studies, there seems to be a strong association of CuV with CTCL.

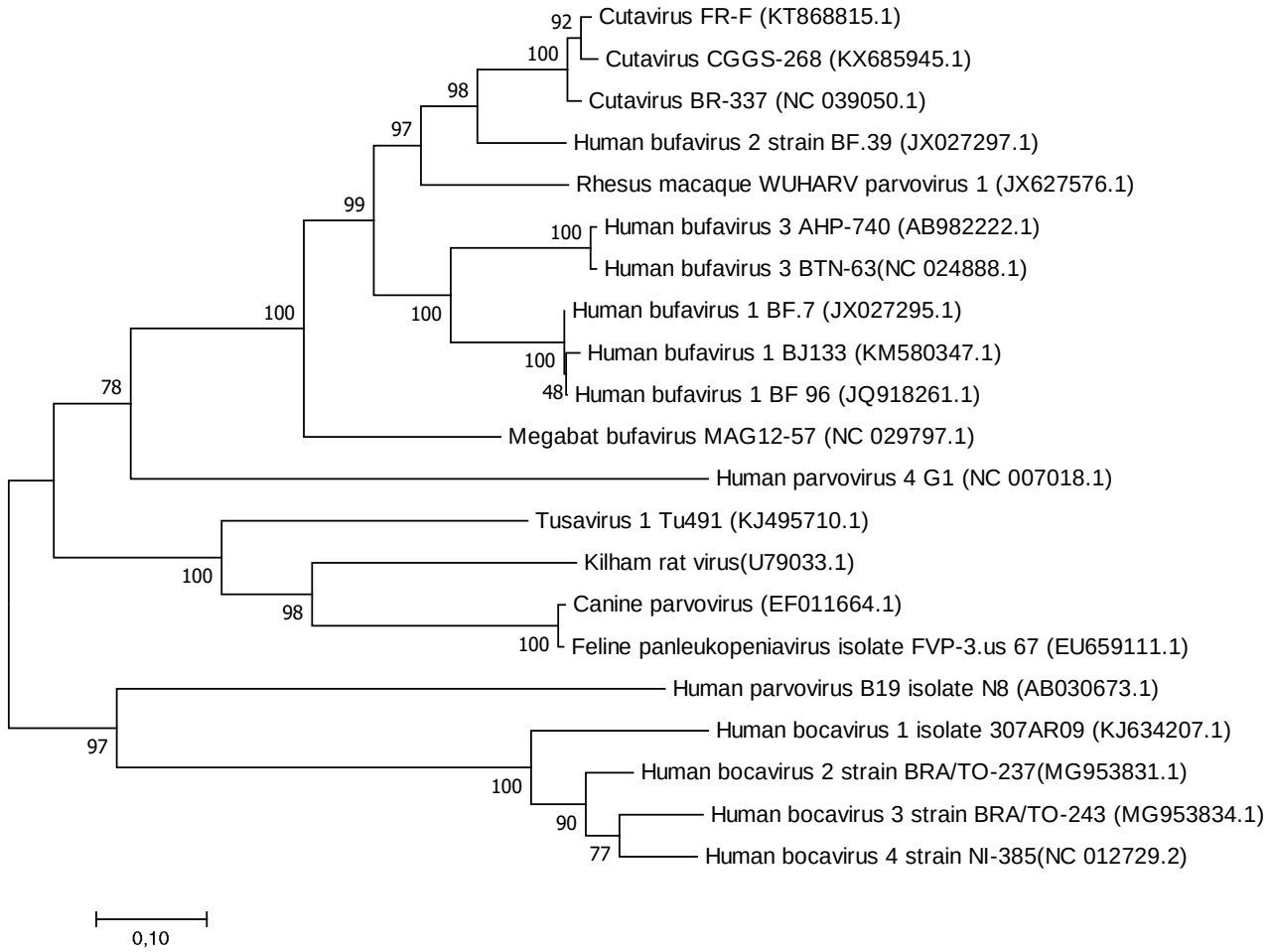


**Figure 5.** Molecular phylogenetic analysis of a group of parvoviruses by the maximum likelihood method based on the virus *VP2* gene nucleotide. The maximum likelihood method is based on the Tamura-Nei model (Tamura & Nei, 1993). The tree was generated with 1000 bootstraps and is drawn to scale, with branch lengths measured in the number of nucleotide substitutions per site. The percentage in which the taxa is clustered is shown next to the branches. Sequences were aligned with ClustalW with open gap penalty of 10 and gap extension penalty of 0.1. Evolutionary analyses were conducted in MEGA7 (Kumar *et al.*,2016).

### *1.2.3. Tusavirus has been found in only one fecal sample*

Tusavirus, corresponding to Tunisian stool-associated parvovirus, was found in Tunisia in 2014 during a metagenomic study (Phan *et al.*, 2014). A near full-length sequence of 4424 bp (GenBank accession no. #KJ495710) was obtained from a stool sample of a small child suffering from unexplained diarrhea. When comparing the sequence with those of other parvoviruses, TuV is more closely related to rodent parvoviruses than to BuV or CuV or other human parvoviruses (Figures 4 and 5). Väisänen *et al*. (2016 and 2018) reported low levels of TuV IgG in two serum samples of a young child and an adult in Finland. Further studies are needed to confirm if TuV is a true human virus.

## 1.3. Principles of qualitative polymerase chain reaction

Polymerase chain reaction (PCR) was invented in 1983 by Kary Mullis (Mullis, 1990) and once the technology was optimized, it completely revolutionized the world of molecular biology. PCR enables exponential amplification of a specific segment of DNA with very high sensitivity and specificity. PCR is based on the DNA molecule's unique nucleotide pairing (A-T and G-C) as well as the ability of the DNA strand to denature and anneal when the temperature is changed. PCR has undisputed attributes when compared to other pathogen identification methods analyzes can be performed within a few hours, it is highly specific and sensitive, it is widely commercialized and the reagents for standard PCR are relatively inexpensive. PCR is a high-throughput method where multiple samples can be analyzed to detect at least three pathogens simultaneously. However, PCR has a few drawbacks. To avoid contamination and false positive results, several precautions need to be taken when performing the assay. All reagents and plastics have to be PCR-sterile and usually several rooms are needed: one for master mix preparation and one for sample handling.

PCR is an effective tool in pathogen DNA detection especially in clinical diagnostics, where speed, specificity and sensitivity are crucial. PCR-based methods are widely used in hospital laboratory diagnostics in Finland to detect viral and bacterial DNA in patient samples (Hus.fi, 2019). PCR-based techniques are extensively utilized in genomic studies, epidemiology, causal connections and distribution of pathogens etc.

### *1.2.1. Quantitative PCR and hydrolysis probe technology*

Real-time quantitative PCR (qPCR) is based on the traditional PCR method, but real-time qPCR allows a real-time quantification of the sample by means of a standard curve and probe. There are two major qPCR technologies: the so-called dye-based method and probe-based methods. In the dye-based methods the dye, such as SYBR Green, is added to the master mix. The dye binds to double-stranded DNA and emits a fluorescence signal. The problem with dye-based methods is the lack of target specificity. The probe-based methods rely on a probe designed specifically to bind the desired target sequence. In this work the hydrolysis-based TaqMan probe format was used. The TaqMan probe is a nucleotide strand from 18 to 30 nucleotides in length, labeled with a fluorophore at the 5' and with a quencher in the 3' end. Simplified, when both fluorophore and quencher are attached to the nucleotide strand, no or very little fluorescence is detected. The quencher suppresses the fluorescence emitted by the fluorophore via fluorescence resonance energy transfer (FRET) when the two molecules are in proximity. If the probe is hybridized to the target sequence and DNA polymerase extends the primer, the probe is hydrolyzed, and the fluorophore is released, whereby the fluorescence

signal can be detected (Figure 6). TaqMan probe is especially beneficial in multiplex qPCR methods, where several individual targets can be detected in a single reaction.

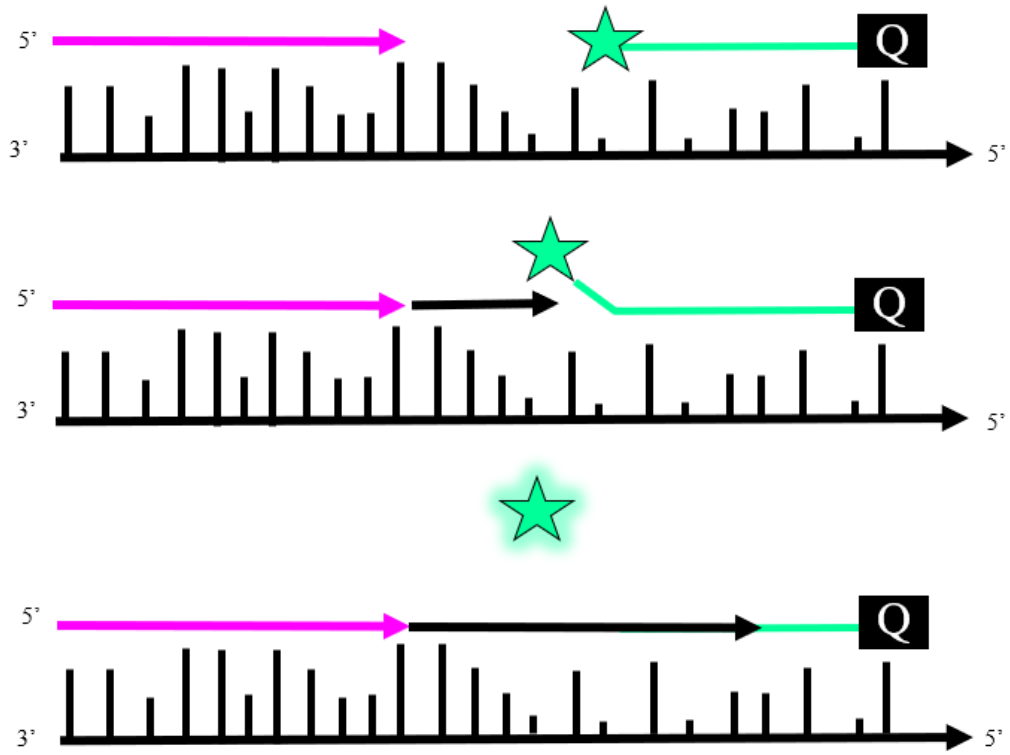


**Figure 6.** Simplified illustration of TaqMan® probe-based PCR assay. Both primer (pink arrow) and probe (green strand) hybridize with the complementary DNA strand. The quencher (Q) suppresses fluorescence when quencher and fluorophore are in proximity. Once DNA polymerase extends the primer, the probe is hydrolyzed, and the fluorophore is released into the reaction mix. The strength of the detected signals corresponds to the amount of amplified sequences.

The BuV, CuV, TuV multiplex qPCR is based on the absolute quantification with a standard curve to calculate the quantity of the viruses in each sample. Absolute quantification is based on the standard curve, which in this case is produced by a dilution series of a plasmid containing the genome region of interest, where the copy number of each plasmid is known in each dilution. The quantification cycle value or $C_q$ value, is the number of cycles that a certain specimen requires to reach the fluorescence threshold value. In this case the standard curve is a plot of the $C_q$ values from each dilution ($10^0$ to $10^6$) and the number of copies assigned to each standard dilution. The number of viral genome copies in each specimen can then be calculated based on the sample's $C_q$ value in qPCR.

## 1.4. Principles of IgM EIA

Immunoglobulins or antibodies are proteins secreted by B-cells of the adaptive immune system. Antibodies are activated during viral infection, when an unknown molecule, an antigen, enters the host. Human antibodies are grouped into five primary classes based on the structure, location and function. IgA is present in mucous membranes and inhibits pathogen adhesion. IgE is involved in allergies and parasite infections. IgD is expressed on the surface of B-cells and is co-expressed with the transient IgM. IgG has multiple functions such as: neutralizing pathogens, immunity and involvement in secondary immune responses. IgM is often the first response when a new antigen is introduced and can quickly activate the complement. In immunoglobulin class switch, the antibody-producing B-cells can switch the class of Ig it produces, from IgM to IgG (Hedman *et al*., 2011). IgG EIA has been developed for CuV, BuV and TuV (Väisänen *et al.*, 2016; 2018), to study past infections and acquired immunity in individuals as well as seroprevalence in different populations. In the literature, there are no reports on IgM EIA to study acute CuV, BuV or TuV infections.

The enzyme-linked immunosorbent assay (ELISA), or EIA, was first described in 1971 by two groups of scientists. Engvall & Perlmann (1971) and Van Weemen & Schuurs (1971) published papers describing the very first EIA techniques. Today EIA is a technique widely used both in research and in diagnostics. For example, in Helsinki University Hospital laboratory (HUSLAB) several EIA-based assays are used in virus and bacterial diagnostics to detect acute or past infections (Hus.fi, 2019). EIA is based on a few basic principles: covalent binding of the antigen or antibody to a solid surface, the exclusive antigen-antibody bond and the detection of antigen-antibody binding through color change.

### *1.4.1. µ-capture IgM EIA*

The µ-capture EIA format is considered to be more sensitive and specific when compared to the direct-EIA format (Wreghitt and Sillis, 1985). In µ-capture EIA the capture antibody (anti-human IgM) is immobilised onto the plastic surface e.g. microtiter plate. The IgM antibodies present in the serum sample bind to the immobilized anti-human IgM. When the biotin labelled antigen is applied, it binds to the corresponding specific antibody (IgM antibody against the virus of interest). When horseradish-peroxidase (HRP) -conjugated streptavidin is added to the mix, it forms a strong non-covalent bond with biotin. A substrate is then added to oxidise the HRP enzyme, resulting in a color change. The reaction is then stopped with an acid. The strength of color is directly proportional to the amount of IgM antibodies against the specific antigen in the sample and can be measured with a spectrophotometer. The scheme of µ-capture EIA is presented in Figure 7.

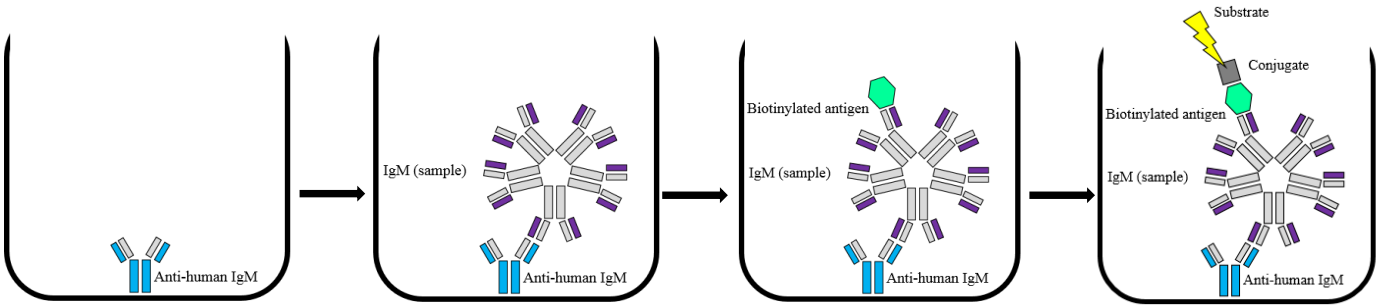


**Figure 7.** Principle of µ-capture EIA presented in a single microtiter well.

Another variant of µ-capture EIA is µ-capture EIA with competition. The competition assay can be used to confirm the positive results of the µ-capture EIA and to rule out cross-reactivity of serum antibodies or background. In competition EIA, the biotinylated and the non-biotinylated antigen competitively bind the antibody (IgM) in the serum. Whether the aim is to verify positive result or to eliminate the possibility of cross-reactivity, the competition assay can be performed with homologous or heterologous antigens. The non-biotinylated antigens are applied in higher concentrations compared to the biotinylated antigens, to maximise the binding of the non-biotinylated antigen. If specific antibodies are present in the sample, the non-biotinylated antigen will bind. Thus, no signal can be detected, since non-biotinylated antigens block the binding sites and the HRP conjugated streptavidin is not able to bind to the non-biotinylated antigen. For example, if the aim is to verify a positive result from µ-capture EIA, the competition assay can be done by competing the sample antibodies with homologous biotinylated and non-biotinylated antigens. If the non-biotinylated antigen binds to the sample, no signal is be detected and the sample can be deemed as positive.

Several factors in the EIA can be optimized: serum dilution, antigen dilutions, substrate incubation time, purity of antigen, used plastics etc. The optimization efforts are more carefully described in materials and methods.

## 2. AIMS OF THE THESIS WORK

There were two main aims in this thesis work:

- To develop and optimize a protoparvovirus IgM μ-capture EIA assay using BuV1 as an example virus. If successful, this assay could be applied for other human protoparvoviruses as well. IgM EIA could be used to find acute protoparvovirus infections and further on investigate the symptoms caused by these viruses in acute infections.
- To screen three patient cohorts for BuV, TuV and CuV DNA with in-house multiplex qPCR to assess viral DNA prevalence within these cohorts and to investigate the distribution of these viruses further.

## 3. MATERIALS AND METHODS

Two main methods were used in the experimental phase of this thesis work: qPCR and IgM µ-capture EIA.

### 3.1. Patient cohorts and sample preparation

Stool or serum samples from four different patient cohorts were used in this study. The cohorts are described in Table 1. The HUSLAB v and b cohorts are collections of fecal samples sent to HUSLAB for norovirus PCR screening and for bacterial PCR screening, respectively. The age range of the patients in both HUSLAB cohorts varied from 0 to 99, mean age 55 years. Both of the HUSLAB cohorts have been previously used and described in (Väisänen *et al.*, 2014). There were 56 samples available from the HUSLAB v cohort and 172 samples from the HUSLAB b cohort. HUSLAB v and b have already been screened for BuV DNA, so only TuV and CuV DNA were screened with duoplex qPCR. The received samples of the Malawi cohort, a collaboration with Per Ashorn from University of Tampere, were purified DNA of fecal samples collected from children 6 or 18 months of age in Malawi for a Child Nutrition Intervention Study (LCNI-5). Some of the samples had dried during storage or there were not enough sample to reach the required 5 µL pipetting volume. In these cases, 5-10 µL of PCR-grade $H_2O$ was added to the sample tube. All stool samples were analyzed in replicates in the multiplex or duplex qPCR, if possible. All the samples were stored at -20 °C.

**Table 1**. Patient cohorts used in the qPCR and/or BuV1 IgM µ-capture-EIA. HUSLAB v and b and MALAWI cohorts were used for BuV, TuV, and CuV -multiplex. The IRAN cohort was used setting up the BuV1 IgM µ-capture-EIA

| Cohort ID | Age | Number and type of samples | Previously described in literature |
|---|---|---|---|
| HUSLAB v | Range: 0-99, median: 55 years | 56 Stool | Väisänen *et al*., 2014 |
| HUSLAB b | Range: 0-99, median: 55 years | 172 Stool | Väisänen *et al*., 2014 |
| Malawi | 6-18 months | 179 Stool | No |
| Iran | Range: 1-77 Median 38 years | 118 Serum | Väisänen *et al*., 2018 |

The samples for the µ-capture IgM EIA consisted of 118 serum samples from Iran, 107 of which were from healthy adults and 11 from children ≥18 years old, with no reported sicknesses. The serum samples were collected in Iran at the Hamadan Blood Transfusion Organization (Hamadan, Iran) and the cohort has been previously described in Väisänen *et al*., 2018. Samples were collected during the years 2015 and 2016 and the age range of the blood donors varied from 1 to 77 years, mean age 39 years. The Iranian cohort was chosen due to the high IgG seroprevalence (over 50 %) for BuV1 (Väisänen *et al.*, 2018).

### *3.1.2. Phenol-chloroform-based DNA extraction*

To validate the IgM-positive EIA results, the serum samples were also studied for BuV DNA by qPCR. For detection of viremia in serum, DNA was extracted from samples which gave over 0.220 absorbance value in the IgM µ-capture assays without blocking (n=40). Phenol-chloroform extraction was chosen, since with this method it is possible to use extremely small amounts of sample material. For the initial extraction step 20 µL of serum, 2 µL of Proteinase K (Thermo Fischer) and Proteinase K buffer were combined and incubated for 30 minutes at +37°C. After incubation, 300 µL of phenol (WVR, pH 8.0) and 200 µL of PCR-grade $H_2O$ was added and the mixture was shortly vortexed and then centrifuged for 2 minutes at 13 000 rpm. The upper phase containing the DNA was transferred into a new microtube and 300 µL of chloroform was added, the mixture was vortexed and centrifuged for 2 minutes at 13 000 rpm. The upper phase was again transferred into a fresh microtube and sodium acetate pH 5.3 was added to a ratio of 1:10. Finally, 1 ml of ice-cold ethanol (WVR) was added and the mixture was shaken vigorously and stored frozen at -20 ºC for approximately 16 hours. After freezing the tubes were centrifuged for 30 minutes at +4 °C with 13 000 rpm. The liquid was carefully removed, and the pellet was dried in a laminar hood. After drying the pellet was suspended into PCR-grade $H_2O$. The purified DNAs were stored at -20 °C.

## 3.2. Multiplex qPCR

An in-house multiplex real-time qPCR for BuV, TuV and CuV has been previously established and published (Väisänen *et al*. 2018). The sensitivity and specificity of the assay is 10 copies of viral DNA/µL with no cross-reactivity between human DNA, B19V, HBoV1-4, PARV4 or 13 human polyomaviruses (Väisänen *et al*., 2018). All samples were analyzed with Agilent Technologies AriaMX real-time qPCR device using disposable 96-well plates (4ti-0740. 4titude) or 8-well strips (4ti-0753/c, 4titude) and flat optical caps (4ti-0751, 4titude). All qPCR master mixes were prepared in a separate clean room prior to handling samples and controls. The samples were handled in a separate sample-handling room. The plasmid controls were applied last in a separate laminar flow cabinet, to minimize contamination. Pipetting to qPCR plates or strips was done in laminar flow cabinets sterilized with 2% Deconex and UV-light.

### *3.2.1. BuV, TuV and CuV -multiplex qPCR assay*

The BuV, TuV, CuV -multiplex assay relies on the TaqMan hydrolysis probe technique (Väisänen *et al*., 2018). Probes for the three viruses were labelled with different fluorescent dyes with unique emission wavelenghts: FAM (~520nm) for BuV, JOE (~552nm) for CuV and Texas Red (~615nm) for TuV. The master mix consists of 1x Maxima probe qPCR Master Mix, without passive the reference dye ROX (Thermo Scientific). ROX was not used as passive reference dye, since the emission wavelength of ROX (~605nm) overlaps with the emission spectra of Texas Red. Maxima probe qPCR Master Mix is ready-to-use and contains Maxima Hot Start Taq DNA polymerase, dNTPs and dUTPs. Primers and probes were added to the Maxima Master Mix as follows: 0.2 µM of BuV and TuV probes, 0.4 µM of CuV probe, 1.0 µM of CuV forward primer and 0.5 µM of all other primers. Primer and probe sequences and amplicon lengths are presented in Table 1. Primers and probes are located in the VP2 (TuV and CuV) or NS1 (BuV) regions (Väisänen *et al*., 2018).

The total volume of each reaction was 25 µL, with 5 µL of the sample template. The qPCR protocol was the following: hot-start at 95 °C for 10 minutes, denaturation at 95 °C for 15 seconds, annealing at 62 °C for 1 minute. Denaturation and annealing were repeated 45 times.

**Table 2.** Primer and hydrolysis probe sequences (‘5- ‘3) and lengths of the amplicons. The names of fluorophores and quenchers are marked in bold.

| Oligo name | Sequence (5’-‘3) | Amplicon length (bp) |
|---|---|---|
| BuV primer forward | ACAGTGTAGACAGTGGATTCAAACTT | |
| BuV primer reverse | GTTGTGGTTGGATTGTGGTTAGTTC | |
| BuV primer probe | **FAM**-CGGAAGAGATTTTGACAGTGCYTAGCAA-**BHQ1** | 126 |
| CuV primer forward | TAACACATCCCAGAATYGTCACATA | |
| CuV primer reverse | TTCCATTGTCTTGGAGTGCG | 118 |
| CuV primer probe | **JOE**-AGTTKTCCTGACCACCAGAAGGTTCCA-**BHQ1** | |
| TuV primer forward | CCAGAAAGCCGTATCACCAT | |
| TuV primer reverse | AACCAAGTGTTTCTGATCTTATTGCT | 91 |
| TuV primer probe | **TxRd**-ACACCAACAATCAACTGCCATACACACC-**BHQ2** | |

*3.2.2. Preparation of the plasmid standard*

Plasmids containing a part of BuV, TuV or CuV genomes were used as positive controls for each run as well as to establish the standard curve for quantification. A 3.5 kb sequence of BuV NS1 region (16-3577 nt, JX027295) , a 1.7 kb sequence of TuV VP2 region (2659 - 4356 nt, KJ495710.1), and a 1.7 kb sequence of CuV VP2 region (2747 - 4456 nt, KT868811) had been previously cloned into the pSTBlue acceptor vector (Novagen) and bacterial glycerol stocks containing the plasmids had been stored at -70 °C. Elina Väisänen inoculated the bacteria from glycerol stocks. Isolation of a single colony, carrying the plasmid, was done to obtain homogenous bacterial suspension for plasmid purification.

The plasmids were extracted with GeneJet Plasmid Miniprep Kit (Thermo Fischer) and the concentration was measured with Nanodrop 1000 Spectrophotometer (Nanodrop, Wilmington, DE) at 260 nm wavelength. The plasmids were verified by restriction digest. *Eco*RI FastDigest restriction enzyme (Thermo Fischer) was used for the CuV and TuV plasmids and *Hind*III (New England Biolabs) for the BuV plasmid. *Eco*RI cuts the CuV and TuV plasmids at two sites, resulting in two fragments with sizes of ~3.8 kb and ~1.7 kb. *Hind*III cuts the BuV plasmid at two sites, resulting in

two fragments with sizes of 1.5 kb and 5.6 kb. All restriction digests were carried out as described in the manual provided by the manufacturer. Restriction digest reactions containing 1 µg of plasmid DNA were carried out overnight at 37 °C and the reactions were inactivated according to the product manuals. To visualize DNA fragments after restriction digest, 5 µL of the reaction mix was added to 1.5 µL MidoriGreen Direct (Nippon Genetics) and applied to agarose gel electrophoresis. The 2 % agarose gel (SeaKem® LE Agarose, Lonza) in TAE-buffer (40 nm Tris, 20 nM Na-acetate, 3 mM EDTA, pH 8.0) was utilized with BIO-RAD PowerPac® power supply at 90 V for 45 minutes. The gel was observed under UV light (BIO-RAD Gel Doc) and stained with ethidium bromide (EtBr) for 45 minutes.

The plasmid copy number/µL was calculated for each control plasmid using the concentration and the molecular weight of the DNA. The copy number/µL of each plasmid was adjusted to $1 \times 10^9$ with TE-buffer (10mM Tris: 0.1mM EDTA; pH 8.0) and 10-fold dilution series was created with TE-buffer until $1 \times 10^0$ copy/µL was reached. Furthermore, a plasmid mix was created by adding 20 µL of each plasmid at $1 \times 10^9$ copies/µL to 140 µL of TE-buffer. The plasmid mix was diluted into a 10-fold dilution series using TE-buffer, until $1 \times 10^0$ copy/µL was reached (Figure 8). The performance of the plasmid mix dilution series was evaluated by comparing it in multiplex qPCR with single plasmid dilution series of CuV, TuV and BuV. Dilutions from $10^6$ to $10^0$ were used for each plasmid. In the final qPCR analyses the plasmid mix dilutions from $1 \times 10^6$ to $1 \times 10^0$ were used to create the standard curve. To ensure the quality of the standard plasmids, dilutions from $10^6$ to $10^0$ were aliquoted and stored at -20°C. Other plasmid preparations were stored at -70°C.

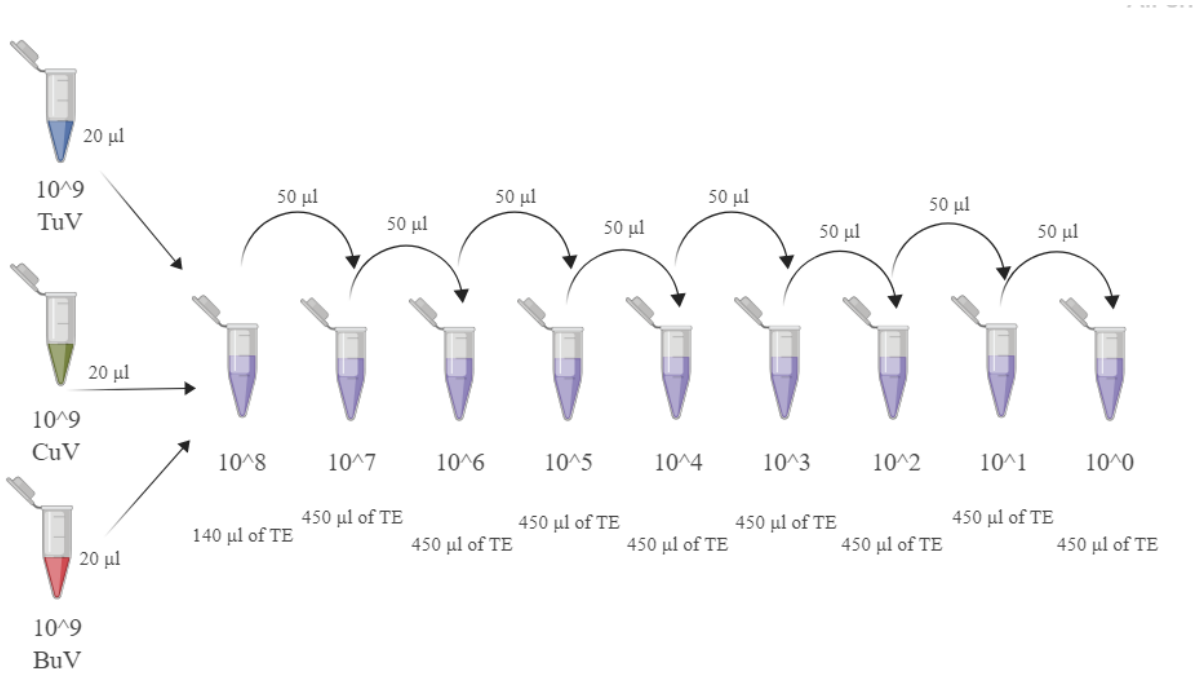

**Figure 8**. Scheme of the 10-fold dilution series of the plasmid mix. Between each dilution the mix was vortexed vigorously with Vortex Genie 2 (Scientific Industries Inc.) to achieve a homogenous mix. Picture created with BioRender (https://biorender.io/).

Preliminary qPCR results were assessed with Agilent Aria 5.1. software to estimate the success of the run. The efficiency and the slope of the standard curve were monitored, the optimum values for each being ~100 and 3.4, respectively. $C_q$ values of each replicate of the plasmid control dilution should vary with maximum 1 cycle. The Agilent Aria 5.1. software calculates the viral load of each sample automatically based on the standard curve.

### *3.2.3. Amplicon sequencing*

The samples that gave a positive result in qPCR for BuV, TuV or CuV were sequenced. For sequencing, the positive amplicons were first re-amplified by using 1 µL of the qPCR product in 4 µL of PCR-grade water as template for singleplex qPCR. Re-amplification was done with the same primers and probe of the virus in question with the same master mix and qPCR program as described before. To check the sequences of the PCR-positive samples, the products from re-amplification were purified with Diffinity RapidTip® (Sigma-Aldrich) to remove primers, probes and dNTPs. The concentration of the purified qPCR products was measured with Nanodrop. The amplicons were prepared for sequencing as advised on the Institute of Molecular Medicine Finland's (FIMM) websites (fimm.fi): 1.6 µL of 5 mM primer and 5.0 µL of the amplified PCR product containing 1-3 ng of DNA. Samples were sent to FIMM for full-service sequencing in duplicates with both reverse and forward primers of the virus corresponding virus (Table 1.).

### *3.2.4. Analysis of the sequencing results*

The sequencing results were first evaluated with SequenceScanner v1.0 software (Applied Biosystems) by observing the fidelity of the chromatogram. Secondly, the sequences, primers and templates were submitted to MultAlin software (http://multalin.toulouse.inra.fr/multalin/) to quickly estimate the correlation between nucleotide sequences. For each qPCR positive sample, sequences gained with both forward and reverse primers were aligned with the template (plasmid sequence) in BioEdit v7.0.5 software. The fidelity of each nucleotide was cross-checked with the chromatogram. The poorly-defined nucleotides or degenerative bases were fixed, when possible, based on the chromatogram and on the overlapping sequence gained with the other primer or according to the

IUPAC code. All sequences were aligned with the corresponding plasmid template to check for possible mismatches. Finally, all sequences were analysed with BLAST (Basic Local Alignment Tool, https://blast.ncbi.nlm.nih.gov/Blast.cgi) to find similarities with known sequences in the National Center of Biotechnology Information database.

## 3.2. Developing the µ-capture IgM EIA for human protoparvovirus

The used IgM µ-capture EIA and competition IgM µ-capture EIA protocols are based on IgM EIAs developed for HBoVs (Söderlund-Venermo *et al.*,2009 and Kantola *et al.*, 2011). Biotinylated and non-biotinylated virus-like particles (VLP) were used as antigens. VP2 of BuV, TuV and CuV can self-assembe into virus-like particles (Ilyas *et al.*, 2018; Väisänen *et al.*, 2016, 2018).

### *3.2.1. Optimizing the BuV1 µ-capture IgM EIA*

Before screening the Iran serum sample cohort with the BuV1 µ-capture IgM EIA, several factors were studied to optimize the assay. First step of optimizing the assay was to test different concentrations of the biotinylated BuV1 VLP antigen. From the Iran cohort, 18 randomly selected serum samples were analyzed with IgM µ-capture EIA using three different antigen concentrations: 10 ng, 20 ng and 40 ng per 100 µL. The chosen antigen concentrations were based on what had previously been used for other parvoviruses in IgG or IgM (Chen *et al.*, 2011; Söderlund-Venermo *et al.*, 2009; Kantola *et al.*, 2011; Riipinen *et al.*, 2010; Väisänen *et al.*, 2018; Väisänen *et al.*, 2016; Maple *et al.*, 2014). Two diluents were compared for the serum dilutions: RED buffer solution (Kaivogen) and Phosphate buffered saline solution (PBS), using 16 randomly selected samples in the Iran cohort. Two different substrate incubation times were tested: 15 min and 20 min.

Based on antigen concentration, serum diluent and substrate incubation testing experiments, the protocol described below was chosen.

### *3.2.1. BuV1 µ-capture IgM EIA*

Costar E.I.A/R.I.A strips were coated with goat antiserum to human IgM (Cappel, MP Biomedicals) with a dilution of 1:1200 in 0.05 M carbonate buffer (bicarbonate buffer capsules, Sigma), pH 9.6. The coating was done at room temperature (RT) (+24 °C) by adding 100 µL of the antiserum dilution to each well. The strips were incubated overnight at RT. After incubation, 100 µL of 3 % bovine serum albumin (BSA) (Sigma-Aldrich) in phosphate-buffered saline (PBS) was pipetted into each well. Strips were incubated for 30 minutes at +37°C. After incubation, wells were washed with PBS and 0.05 % Tween 20 (PBST) buffer. Finally, the dried strips were stored at -20 °C until use.

The serum samples were diluted 1:200 into RED buffer solution (Kaivogen) and each sample was applied to pre-coated wells in duplicates, 100 µL per well. Serum dilutions were incubated for 60 minutes at RT with 400 rpm shaking. Wells were rinsed five times with 300 µL of PBST. Biotinylated BuV1 VP2-VLP antigen was diluted into PBST with 0.5 % BSA to the desired concentration of 10 ng, 20 ng or 40 ng per 100 µL. The diluted antigen was applied to the wells, 100 µL into each, and the mixture was incubated for 45 minutes at +37 °C without shaking. After antigen incubation, wells were washed as described before. Peroxidase-conjugated streptavidin (Dako) was diluted 1:12000 into PBST with 0.05 % BSA, 100 µL of the dilution was distributed into each well. Strips were incubated and washed as described in the previous step. After the conjugate incubation, 100 µL of 3,3′,5,5′-Tetramethylbenzidine (TMB) substrate (Sigma) was dispensed to each well. Substrate was incubated for 15 or 20 minutes at +37 °C. To stop the reaction, 100 µL of 0.5 M sulfuric acid $H_2SO$ (Fluka) was added to each well. Absorbance was measured with a wavelength of 450 nm (Multiskan EX, Thermo Labsystems). A strip with 100 µL of TMB substrate and 100 µL of sulfuric acid was used as a blank. The blank value was subtracted from the test results. No BuV1-IgM positive or negative serum sample was available to be used as a control. Instead, well-characterized B19V-IgM positive and negative serum samples were used as technique and reagent controls for each assay in B19V VP2 µ-capture IgM EIA (Maple *et al.*, 2014).

### *3.2.2. BuV1-3 and CuV µ-capture competition IgM EIA*

To verify the specific IgM to BuV1 antigen and to rule out possible cross-reactivity to BuV2-3 and CuV antigens, µ-capture competition IgM EIA was performed in a set of serum samples that were considered putatively positive in BuV1 µ-capture IgM EIA. A total of six serum samples were tested with competition EIA for all BuVs (1-3) and CuV. Each serum was assigned to homologous and heterologous competition with three VLPs and one well was assigned to no competition treatment. Two non-biotinylated antigen concentrations, 20 µg and 30 µg per well, were tested in two separate µ-capture competition IgM EIAs.

The antiserum-coating of the wells, serum incubation and the first wash were done as described for the BuV1 µ-capture IgM EIA. To maximize the binding of the non-biotinylated antigen, a pre-incubation was done with 100 µL PBST containing 0.5 % BSA or with 100 µL of the non-biotinylated antigen (20 µg or 30 µg per ml) diluted into PBST with 0.5 % BSA. The pre-incubation was done at +4 °C for 1.5 hours. After the pre-incubation, the mixtures were removed by suction. Next, 100 µL of the biotinylated VLPs (20 ng per well) or a mixture of biotinylated VLPs (20 ng per well) and non-biotinylated homo- or heterologous VLPs (20 µg or 30 µg per ml) were applied to the wells. The

mixtures were incubated for 45 minutes at +37 °C. Washing, substrate incubation, termination of the reaction, blank strip preparation and the absorbance measurement was conducted as described for BuV1 IgM µ-capture EIA.

If the sample has IgM antibodies for a specific antigen the signal is blocked after incubation with homologous non-biotinylated antigen, whereas incubation with heterologous non-biotinylated antigens should not block the specific reaction. The absorbance value measured in the no competition well should correspond to the µ-capture IgM EIA result.

### *3.2.3. Troubleshooting the µ-capture IgM EIA*

To troubleshoot the µ-capture IgM EIA, different variables of the assay were studied. It was investigated whether storage of the pre-coated strips affect the IgM binding performance of the goat antiserum to human IgM. Strips after 1 year, 3 months, 10 days and 1 day of storage were compared. The performance of streptavidin used in all the assays was compared with a fresh streptavidin. The strips and streptavidin conjugate were tested using the well-characterized B19-IgM positive and negative serum samples, which were used as technique and reagent controls in BuV1 µ-capture IgM EIA, as well as Sample N30 from the Iran serum sample cohort. The B19-positive and negative samples were tested with B19 VP2 µ-capture IgM, with antigen concentration of 10 ng/well. The sample N30 was tested with the BuV1 µ-capture IgM EIA, with antigen concentration of 10 ng/well.

Finally, the used VLPs were examined by producing new biotinylated and non-biotinylated VLPs and comparing the performances of the different VLP batches in IgM and IgG.

### *3.2.4. Production and purification of CuV VP2 VLPs*

VLPs were produced as the final attempt to troubleshoot the IgM EIA. Instead of producing BuV1 VLPs, CuV VP2 VLPs were chosen due to the incoherent results with CuV VLPs in IgM competition EIA.

For CuV VP2 VLP production, High five insect cells were thawed from liquid nitrogen storage and suspended into Xpress insect cell media (Lonza Biosciences) with 10 % fetal bovine serum (FBS) (Gibco). The cells were let to attach to the T25 flask bottom for one hour after which the media was changed to new, in order to remove any residual of dimethyl sulfoxide (DMSO) present in the storage media. The cells were grown in T25 flasks (Sigma-Aldrich) at +27 °C. Cells were passaged every 2 to 4 days and were transferred during the first passages from the T25 flask to a T75 (Sigma-Aldrich) flask and finally to a T175 (Sigma-Aldrich) flask. Amphotericin B, penicillin and streptomycin were

gradually added during the first passages. The amount of antibiotics was increased by 20 % in during each passage, until the final concentrations of 25 µg/ml of amphotericin B, 100 U/ml of penicillin and 100 µg/ml of streptomycin were reached. When the growth of the culture reached a stable state and the cells were adjusted to the final concentration of antibiotics, the cells were split into 1:10 creating several parallel cultures in T175 flasks.

Before infection the cells were split to 1:7 and incubated overnight. The insect cells were infected with 500 µL of passage 3 media of recombinant baculovirus, containing the CuV *VP2* gene (Väisänen *et al.*, 2018). The infected cells were cultivated in a separate infection room at +27 °C. The culture was followed every day and on average 4-6 days post infection, the cells were visibly dead i.e. detached from the bottom of the flask. On average, 24-30 T175 flasks were infected simultaneously. The detached cells were collected by centrifuging for 5 minutes at 4000 rpm (Heraeus, Megafuge 10). The cell pellet was resuspended into approximately 30 ml of 20 mM Tris-HCl with 2x EDTA-free protease-inhibitor (Roche) with 0.5 % deoxycholic acid (DOC) (Sigma-Aldrich). The mixture was distributed into 15 ml Falcon tubes and incubated at +37 °C with mild shaking for 30 min and chilled on ice for 15 minutes. Cells were sonicated with an ultrasonic probe sonicator (Bandelin, Sonoplus) with the following program: 10 s agitation + 10 s pause for eight times with 50% amplitude. During sonication the cell tube was immersed in an ice bath to prevent heating. After sonication the cells were centrifuged with full speed (Eppendorf Centrifuge 5415 R) for 30 minutes at +4 °C. The supernatant was collected, and the pellet was resuspended into 20 mM HCl-Tris with 2x EDTA-free protease -inhibitor. Sonication and centrifugation were repeated.

The VLPs were purified by caesium chloride (CsCl) ultracentrifugation. A double cushion of CsCl was created by preparing a CsCl Solution 1 with a density of 1.52 g/cm3 (heavy). The CsCl powder was dissolved into TE-buffer. Solution 2 was created diluting Solution 1 with TE-buffer with a ratio of 57:43 resulting in a final density of 0.653 g/cm3. A double cushion was created into each ultracentrifuge tube (Beckman&Coulter) by carefully pipetting in the following order from bottom to top: 7 ml of Solution 1, 11 ml of Solution 2, ~15 ml of cell lysate and, if needed, the tube was filled to the top with TE. Depending on the growth of the cells, pellets from 4-7 cells flasks were pipetted to each centrifuge tube. The lysates were then centrifuged for 16 hours, 26 000 rpm, +10 °C (Beckman L-70).

During ultracentrifugation VLPs formed a visible band, which was collected to microtubes. Approximately 4-6 ml of VLPs were collected from each ultracentrifuge tube. To ensure maximum purity, the ultracentrifugation was repeated. Between ultracentrifuge purifications, VLPs were dialysed against PBS for 6 hours to remove CsCl. The final purified product was further dialysed

against PBS for 18 to 24 hours changing PBS every 6 to 8 hours. The dialyses were done at +4 °C with constant mixing. After ultracentrifugation VLPs were analysed on sodium dodecyl sulphate–polyacrylamide gel electrophoresis (SDS-PAGE) (10% acrylamide/bis) at 90 V for 1.5, hours with Precision Plus Protein™ Dual Colour Standard as standard. If needed, the VLPs were concentrated with Amicon Ultra Centrifugal Filter Units. Concentration of the VLPs was measured with Pierce BCA Protein Assay Kit (Thermo Fischer). Biotinylation of the VLPs was done with EZ-Link® Sulfo-NHS-LC-Biotin (Thermo Fischer) with 20-fold molar excess of 10 mM biotin according to the manufacturer's instructions. The unbound biotin was removed by dialysis. The biotinylated VLPs were stored at -20 °C in PBS with 0.5 % sodium azide ($NaN_3$), 4 mg/ml BSA, 50 % glycerol and 4 % EDTA -free protease inhibitor (Roche) in PBS. The non-biotinylated VLPs were stored at +4 °C with 0.5 % $NaN_3$.

The performance of the biotinylated and non-biotinylated CuV VP2 VLPs were tested in non-competition and competition IgG EIA (Väisänen *et al.*,2016) using a known BuV1-3 -positive serum sample with CuV cross -reactivity and known CuV -positive and -negative serum samples. Briefly, 80 ng/well and 160 ng/well of the biotinylated CuV VLPs were diluted in PBST and applied to streptavidin-coated plates (UniverSA96-Lockwell, Kaivogen). The plate was incubated for 1 hour at RT with 400 rpm shaking. Plates were post-coated with the Diluent (Labsystems Diagnostics) 3 times for 10 minutes 150 µL/well. The serum samples were diluted 1:200 in RED buffer and incubated for 1 hour at RT with 400 rpm shaking. The wells were washed with 300 µL of PBST 4 times within 15 minutes. A secondary-antibody HRP-conjugated anti-human IgG (DAKO, #P124) was diluted 1:4000 in the Diluent and applied 100 µL per well. The secondary conjugated -antibody was incubated for 1 hour at RT with 400 rpm shaking. Wells were washed with PBST as previously. TMB was used as substrate and the reaction was stopped with $H_2SO$. For the competition assay the serum samples were pre-incubated with non-biotinylated antigen for 1.5 h at +4 °C, using CuV and BuV2 VLPs. Results were measured as described for IgM EIA.

## 4. RESULTS

The aims of this thesis were to screen three patient cohorts for BuV, TuV and CuV DNA with in-house multiplex qPCR and to develop an IgM EIA for human protoparvoviruses using BuV1 as an example.

### 4.1.Multiplex qPCR

#### *4.1.1. The plasmid standard*

To verify that all the extracted plasmids were holding the correct insert, restriction analyses were done in duplicate reactions (A and B) for each plasmid. The plasmid containing a part of the BuV genome was digested with *Hind*III restriction enzyme. *Hind*III cuts the BuV plasmid at two sites resulting in fragments with expected sizes of ~1.5 kb (part of the insert) and ~5.6 kb (part of the insert + vector backbone). The plasmids containing a part of the CuV or TuV genome were digested with *Eco*RI restriction enzyme, which cuts both plasmids into two fragments: ~1.7 kb (insert) and ~3.8 kb (plasmid backbone). Analysis of the digested plasmids by agarose gel electrophoresis are presented in Figure 9. Plasmids BuV A and B, TuV A and B and CuV A were cut as expected and resulted in correct sized fragments. Fragments for the digested plasmid CuV B were observed to be shorter than expected. It was evaluated that CuV B plasmid was not cut correctly and it was not used for the plasmid standard dilutions.

Plasmids BuV B, TuV A and CuV A were chosen for the plasmid standard dilutions. Concentrations of the plasmids were measured with Nanodrop: 378 ng/µL for the BuV plasmid, 198 ng/µL for the TuV plasmid and 168 ng/µL for the CuV plasmid.

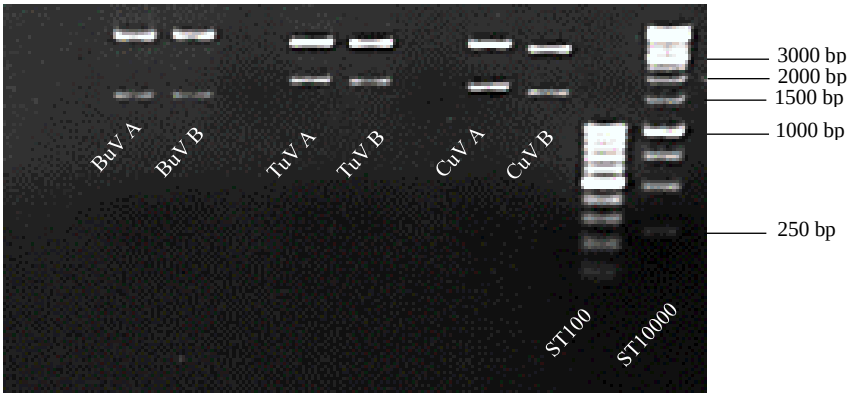


**Figure 9**. Analysis of restricted plasmids BuV, TuV and CuV by agarose gel electrophoresis. From left to right: restricted BuV plasmids A and B, restricted TuV plasmids A and B and restricted CuV plasmids A and B. For BuV the fragment sizes were as expected: ~5.6 kb and ~1.5 kb. TuV A and B as well as CuV A plasmid restrictions had correct sizes after the restriction analysis: ~1.7 kb and ~3.8 kb. The used size standards are on the right side of the picture: Generuler ladders 100 bp (ST100) and 1 kb (ST1000) (Fermentas). Sizes for the 1 kb ladder are presented on the right side of the ladder.

Each plasmid was diluted in a 10-fold dilution series from $1 \times 10^9$ to $10^0$ copies/µL. In addition to that, a plasmid mix was created by combining the $1 \times 10^8$ copies/µL dilution of each plasmid. The mix was further on diluted as a 10-fold dilution series until $1 \times 10^0$ copy/µL was reached. The aim was to use the plasmid mix to create the quantification standard for the qPCR. Before sample analysis, the performance of the plasmid mix was compared with the single plasmid dilutions to ensure correct quantification. For this, all single plasmid and the plasmid mix dilutions from $1 \times 10^0$ to $10^6$ copies/µL were analyzed with the BuV, TuV, and CuV –multiplex qPCR in a single qPCR assay. The $C_q$ values from each individual plasmid dilutions were compared to each other as well as to the $C_q$ values of the plasmid mix. As is visualized in Table 3, all single plasmid and plasmid mix dilutions have similar $C_q$ values when compared to each other. Based on this assay, the plasmid mix dilutions from $1 \times 10^0$ to $10^6$ copies/µL were used to create the quantification standard for the sample analysis. Mean $C_q$ values and standard deviations are calculated from two replicates of each dilution.

**Table 3.** DNA quantification from single plasmid dilutions and the plasmid mix dilutions from $1 \times 10^0$ to $10^6$ copies/µL. Mean $C_q$ values and standard deviations were calculated from two replicates of each dilution.

| | | **BuV average Cq** | | | | **CuV average Cq** | | | | **TuV average Cq** | | | |
|---|---|---|---|---|---|---|---|---|---|---|---|---|---|
| **Dilution** | **Copies/µl** | BuV | | Mix | | CuV | | Mix | | TuV | | Mix | |
| $10^0$ | 1 | 36,68 | ±0,85 | 36,58 | ±0,48 | 35,85 | ±0,42 | 35,70 | ±0,36 | 35,35 | ±0,53 | 35,17 | ±0,55 |
| $10^1$ | 10 | 34,46 | ±0,11 | 33,45 | ±0,07 | 33,52 | ±0,09 | 33,08 | ±0,50 | 33,82 | ±0,34 | 32,93 | ±0,34 |
| $10^2$ | 100 | 30,79 | ±0,08 | 30,27 | ±0,02 | 29,87 | ±0,12 | 29,66 | ±0,08 | 29,87 | ±0,04 | 29,48 | ±0,17 |
| $10^3$ | 1000 | 27,19 | ±0,02 | 27,01 | ±0,15 | 26,42 | ±0,09 | 26,69 | ±0,20 | 26,59 | ±0,04 | 26,41 | ±0,14 |
| $10^4$ | 10000 | 23,75 | ±0,15 | 23,64 | ±0,05 | 23,09 | ±0,15 | 23,28 | ±0,08 | 23,03 | ±0,06 | 22,91 | ±0,12 |
| $10^5$ | 100000 | 20,34 | ±0,04 | 20,18 | ±0,07 | 19,72 | ±0,08 | 19,67 | ±0,05 | 19,83 | ±0,06 | 19,63 | ±0,04 |
| $10^6$ | 1000000 | 17,23 | ±0,01 | 16,76 | ±0,07 | 16,37 | ±0,06 | 16,53 | ±0,06 | 16,64 | ±0,02 | 16,39 | ±0,08 |

*4.1.1. All three viruses were identified in the stool sample cohorts*

A total of 407 stool samples from Malawi, HUSLAB b and v cohorts were screened with BuV, TuV and CuV multiplex qPCR. All samples were analyzed as duplicates, except for the HUSLAB v cohort, for which there was enough sample for only one qPCR reaction. The qPCR analyses included a total of 170 negative controls, PCR-grade water, all of which were negative. The screening of the Malawi, HUSLAB v and b cohorts revealed a total of 2/407 samples positive for BuV DNA (0.5 %), 2/407

samples positive for TuV DNA (0.5 %) and 13/407 samples positive for CuV DNA (3.2 %). Summary of all qPCR screened fecal DNA preps is presented in Table 4.

**Table 4.** Summary of all the BuV, TuV, CuV qPCR -positive samples grouped by the detected virus and cohort.

| | Total number of positives | Cohort ID | Positives/ total | Positives % |
|---|---|---|---|---|
| **BuV** | 2 | HUSLAB B | 1/172 | 0,6 |
| | | MALAWI | 1/179 | 0,6 |
| **TuV** | 2 | HUSLAB B | 2/172 | 1,2 |
| **CuV** | 13 | HUSLAB B | 1/172 | 0,6 |
| | | HUSLAB V | 3/56 | 5,4 |
| | | MALAWI | 9/179 | 5,0 |

BuV DNA was found in one stool sample in the HUSLAB b cohort (1/172, 0.6%) and in one stool sample in the Malawi cohort (1/179, 0.6%). Both samples were BuV DNA qPCR-positive in two out of two replicates. The viral load range of the stool samples was $1.5 \times 10^4$ - $1.2 \times 10^3$ copies/ml (Figure 10), average $7.9 \times 10^3$ copies/ml. The BuV DNA-positive stool sample in the HUSLAB b cohort has been previously identified as BuV DNA-positive and has been published in Väisänen et al., 2014. This sample was not sequenced and is not included in the analyses. QPCR analysed initially gave a positive signal for TuV DNA in two stool samples. Both of the TuV DNA-positive samples belonged to the HUSLAB b cohort (2/172, 1.2%) and were positive only in one of the two replicates. The DNA quantities in the stool samples were $3.9 \times 10^2$ and $1.0 \times 10^2$ copies/ml (Figure 10). A total of 13 stool samples were CuV DNA-positive of which, one was from the HUSLAB b cohort (1/172, 0.6%), three were from the HUSLAB v cohort (3/56, 5.4%) and nine were from the Malawi cohort (9/179, 5.0%). From the 13 CuV DNA-positive stool samples five were positive in two out of two replicates and eight were positive for CuV DNA in one out of two replicates. The viral loads of the samples varied from $4.1 \times 10^4$ to $3.8 \times 10^2$ copies/ml (Figure 10), median $8.5 \times 10^3$ copies/ml.

All stool samples positive for TuV and CuV DNA in qPCR were sequenced as well as the BuV DNA qPCR-positive stool sample from the Malawi cohort.

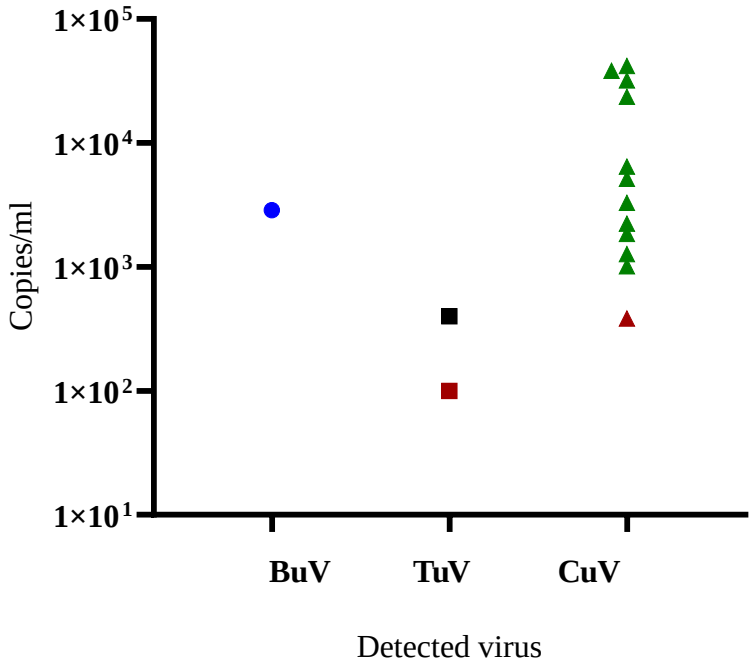


**Figure 10.** Viral loads detected in the fecal DNA preps from all the cohorts grouped by the detected virus. On the y-axis are copies/µL in log10. For each sample, an average viral load was calculated from the positive replicates. On the x-axis are all qPCR-positive samples grouped by the detected virus. Two samples that gave a positive result in the qPCR are marked with red (one TuV and one CuV DNA positive), see chapter 4.1.2.

*4.1.2. Sequencing results*

All samples, which gave a positive signal for BuV, TuV or BuV in the multiplex qPCR were sequenced with both forward (fwd) and reverse (rev) primers of the detected virus. Sample 2 in the Malawi stool sample cohort gave a qPCR-positive signal for BuV DNA (1/407) in both replicates. Sequencing yielded good quality data with both primers with lengths of 88 (fwd) and 89 (rev) bases (Figure 13). Two mismatches can be detected when compared to BuV-1 strain BF.7 (plasmid target sequence), from 5' to 3' G=A and G=A (Figure 11). BLAST analysis revealed that Sample 2-derived amplicon sequence had a 99 % identity with BuV-1 isolate H232 (KU362761.1), BuV-3 strain BJ2180/BeiJing/2014 (KM580355.1), BuV-3 strain BJ189/BeiJing/2011 (KM580352.1) and BuV-2 strain BF.39 (JX027297.1). The BLAST analysis was conducted with standard parameters.

A total of 2/407 samples gave positive signals for TuV DNA in multiplex qPCR, 13FV73 and 13FV10 in the HUSLAB b cohort. Both samples were positive in only one replicate in qPCR and were sequenced. For Samples 13FV73 and 13FV10 the gained sequences, with fwd and rev primers, were

135 bp, 134 bp, 302 bp and 293 bp, respectively. The TuV amplicon length is 118 bp. Sequences from the Sample 13FV73 –derived amplicon were approximately 20 nucleotides longer than the expected TuV amplicon and had 6 mismatches when compared to the plasmid target sequence (TuV1 Tu491) (Figure 11). The sequenced amplicon from Sample 13FV73 was analyzed with BLAST and had a 95 % sequence identity with TuV sp. isolate T.2VLP (KX856940.1) and TuV1 strain Tu491 (KJ495710.1). Sequence data obtained from the Sample 13FV10 –derived amplicon was of bad quality and the gained sequences did not match the expected amplicon in length nor did the sequences match the TuV plasmid target sequence. From the sequence gained with the TuV fwd primer, perfect matches for TuV rev and CuV rev primers sequences were found and from the sequence gained with the TuV rev primer, TuV fwd sequence were identified. Both Sample 13FV10 –derived amplicon sequences with rev and fwd primers were analyzed by BLAST with standard parameters and the sequences share, respectively, an identity of 84 % and 86 % with *Alistipes shahii* WAL 8301 draft genome (FP929032.1). *Alistipes* is a genus in phylum *Bacteroides*, an anaerobic bacteria that can inhabit the human gut (Song *et al.*, 2006). Therefore, sample was not considered positive for TuV DNA. A total of 0.25 % of all analysed samples were positive for TuV DNA.

**A.**

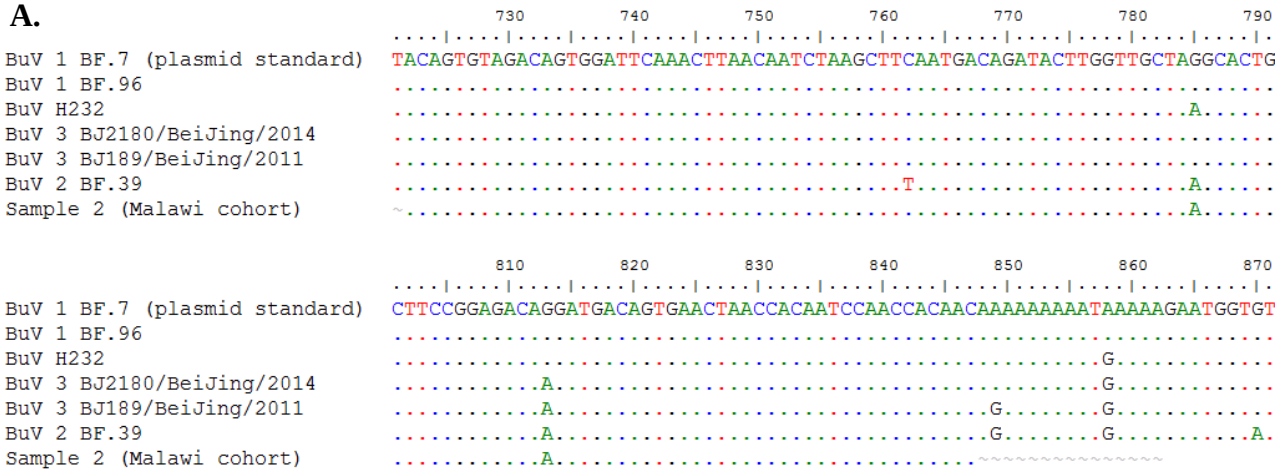
730 740 750 760 770 780 790
BuV 1 BF.7 (plasmid standard) TACAGTGTAGACAGTGGATTCAAACTTAACAATCTAAGCTTCAATGACAGATACTTGGTTGCTAGGCACTG
BuV 1 BF.96
BuV H232
BuV 3 BJ2180/BeiJing/2014
BuV 3 BJ189/BeiJing/2011
BuV 2 BF.39
Sample 2 (Malawi cohort)
810 820 830 840 850 860 870
BuV 1 BF.7 (plasmid standard) CTTCCGGAGACAGGATGACAGTGAACTAACCACAATCCAACCACAACAAAAAAAAATAAAAAGAATGGTGT
BuV 1 BF.96
BuV H232
BuV 3 BJ2180/BeiJing/2014
BuV 3 BJ189/BeiJing/2011
BuV 2 BF.39
Sample 2 (Malawi cohort)

**B.**

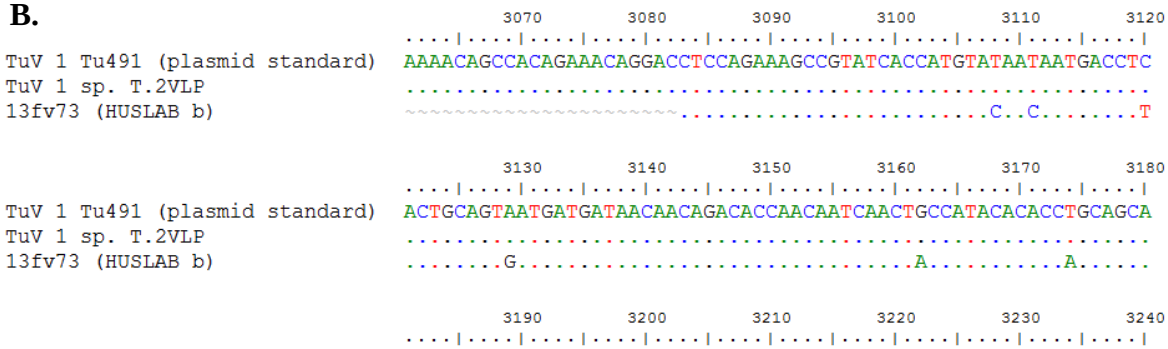
3070 3080 3090 3100 3110 3120
TuV 1 Tu491 (plasmid standard) AAAACAGCCACAGAAACAGGACCTCCAGAAAGCCGTATCACCATGTATAATAATGACCTC
TuV 1 sp. T.2VLP
13fv73 (HUSLAB b)
3130 3140 3150 3160 3170 3180
TuV 1 Tu491 (plasmid standard) ACTGCAGTAATGATGATAACAACAGACACCAACAATCAACTGCCATACACACCTGCAGCA
TuV 1 sp. T.2VLP
13fv73 (HUSLAB b)
3190 3200 3210 3220 3230 3240
TuV 1 Tu491 (plasmid standard) ATAAGATCAGAAACACTTGGTTTTTATCCATGGAGACCTACTGTAGTGCCTAGATGGAGA
TuV 1 sp. T.2VLP
13fv73 (HUSLAB b)

**C.**


4210 4220 4230 4240 4250 4260
CuV BR-337 (plasmid standard) AAAACTAGCACCAAACTATACAGACACACTTGACAACGGAGGTGTAACACATCCCAGAAT
CuV CGG5-268
CuV BR-372
CuV FR-F
29 (Malawi)
36 (Malawi)
37 (Malawi)
68 (Malawi)
76 (Malawi)
129 (Malawi)
146 (Malawi)
181 (Malawi)
2261 (HUSLAB v)
2292 (HUSLAB v)
2299 (HUSLAB v)
13FV38 (HUSLAB b)

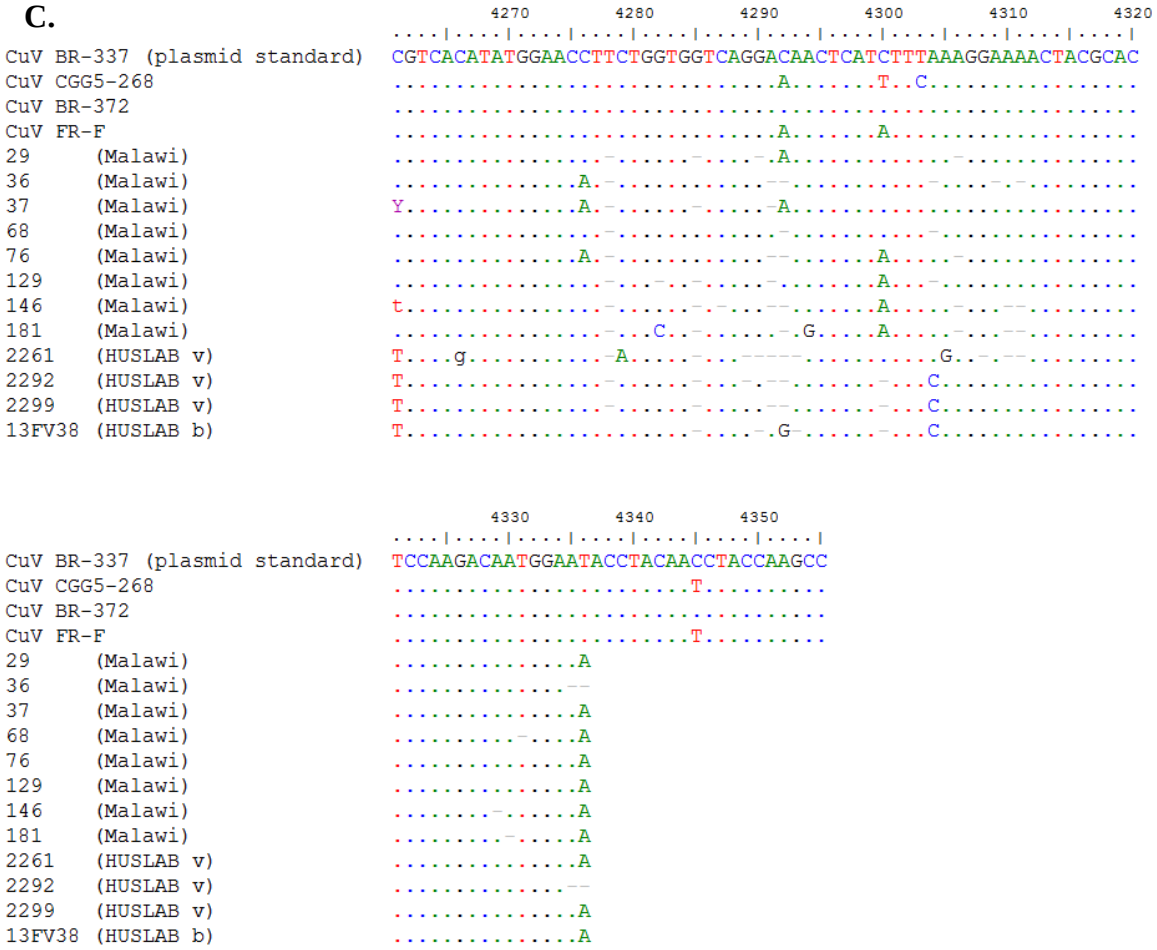


**Figure 11.** Alignment of all the sequenced qPCR-amplicons from BuV, TuV or CuV DNA-positive stool samples. **A.** BuV sequences from top to bottom: BuV2 BF. 39 (JX027297.1) (the plasmid target sequence), BuV1 strain BF.96 (JQ918261.1), BuV isolate H232 (KU362761.1), BuV3 strain BJ2180/BeiJing/2014 (KM580355.1), BuV3 strain BJ189/BeiJing/2011 (KM580352.1), BuV2 strain BF.39 (JX027297.1) and Sample 2 (Malawi cohort). **B.** TuV sequences from top to bottom: TuV1 Tu491 (KJ495710.1) (plasmid standard target sequence), TuV sp. T.2VLP (KX856940.1) and Sample 13FV73 from the HUSLAB b cohort. **C.** CuV sequences from top to bottom: CuV BR-337 (NC_039050.1) (the plasmid target sequence), CuV CGG5-268 (KX685945.1), CuV BR-372 (KT868809.1), CuV FR-F (KT868815.1), Samples 29, 36, 37, 68, 76, 129, 146, and 181 from the Malawi cohort, Samples 2261, 2291 and 2299 from the HUSLAB v cohort and Sample 13FV38 from the HUSLAB b cohort. All sequences are presented as '5 to 3', sequences aligned with BioEdit v7.0.5 software. Dot (.) indicates identical nucleotides, a line (-) indicates an unidentified nucleotide.

A total of 13/407 samples gave a positive signal for CuV DNA in the multiplex qPCR. Samples 68, 76, 129 and 146 in the Malawi cohort and the Samples 2299 and 13FV38 in the HUSLAB v and b cohorts gave positive signals in both qPCR replicates. Samples 29, 36, 37, 54 and 181 in the Malawi and Samples 2261 and 2292 in the HUSLAB v cohort were positive in only one qPCR replicate. Sequencing yielded relatively good quality data for all the sequenced amplicons, except for the amplicon derived from Sample 54 in the Malawi cohort. The CuV amplicon is only 91 bps long, so sequences gained with fwd and rev primers had only little overlap. For samples 37, 76, 2261, 2292, 2299 and 13FV38 the overlapping part was so short that it resulted in a gap in the middle of the analyzed sequences. All samples have a few mismatches when compared to the CuV target sequence (CuV BR-337) (Figure 11.). Samples 29, 36, 37, 68, 76, 129, 146 and 181 in the Malawi cohort and Samples 2261, 2292, 2299 and 13FV38 in the HUSLAB v and b cohorts, respectively, were identified positive for CuV DNA. For Sample 54 the obtained sequences were 154 (fwd) and 153 (rev) bases in length, which is not correct for the CuV target amplicon. Furthermore, the sequences did not match the CuV plasmid target sequence. A near-perfect match for BuV fwd and BuV rev primer sequences can be found from the sequences gained with the CuV rev and CuV fwd primers, respectively. Both sequences were analyzed by BLAST. The sequence acquired with the rev primer gave no results, whereas Sample 54 derived amplicon sequence with fwd primer shared a sequence identity of 95 % with the BuV isolate H232 (KU362761.1), BuV3 strain BJ2180/BeiJing/2014 (KM580355.1), BuV3 strain BJ189/BeiJing/2011 (KM580352.1) and BuV2 strain BF.39 (JX027297.1), which indicates that Sample 54 in the Malawi cohort is not positive for CuV, but in fact for BuV DNA.

## 4.2.The µ-capture IgM EIA

### *4.2.1. Optimizing the BuV1 µ-capture IgM EIA*

Before screening the Iran serum sample cohort with BuV1 µ-capture IgM EIA, three different concentrations, 10, 20, and 40 ng per well, of the biotinylated BuV1 VLP antigen were tested with 18 randomly selected serum samples in the Iran cohort (Figure 12). For the 10 ng per well concentration BuV1 IgM absorbance values varied from 0.054 to 0.181, median 0.095. Absorbance values with the 20 ng per well concentration varied from 0.101 to 0.309, median 0.160 and with the 40 ng per well concentration from 0.185 to 0.605, median 0.309. The calculated cutoff absorbance value for a putatively positive sample in the HBoV1 µ-capture IgM EIA is 0.131 (Kantola *et al.*, 2015) and 0.100 in the BuV1-3 and CuV IgG EIA (Väisänen *et al.*, 2016). Based on these cutoff values, it was evaluated that the 40 ng per well antigen concentration gave excessively high absorbance values. It was decided that BuV1 VLP antigen concentrations of 10 and 20 ng per well will be used to screen the whole Iran serum sample cohort. In addition, the substrate incubation time was lowered to 15 minutes.

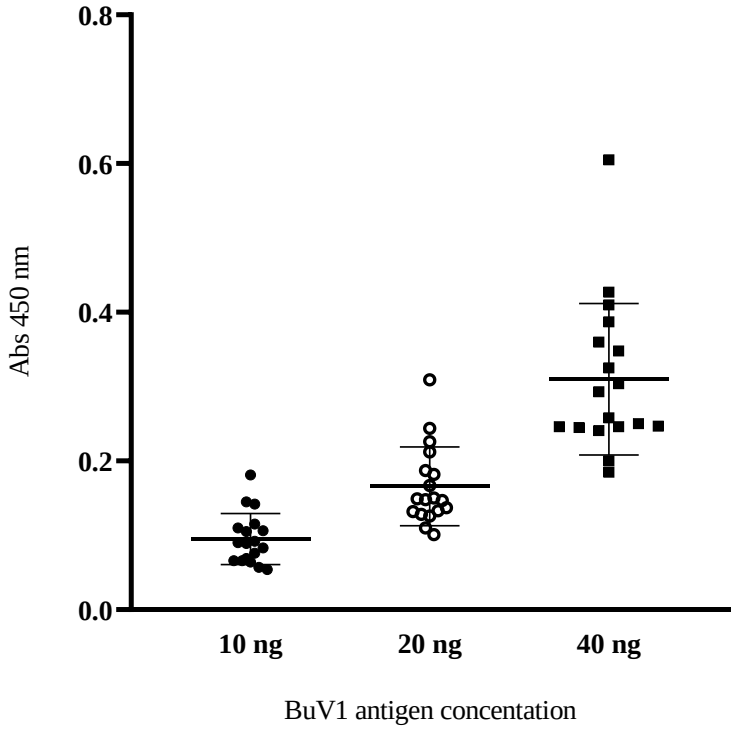


**Figure 12.** BuV1 µ-capture IgM EIA using 18 randomly selected serum samples from the Iran cohort analyzed with three different concentrations of biotinylated BuV1 antigen: 10, 20 and 40 ng per well. The absorbance values are grouped based on the used antigen concentration. Median absorbance values are marked with thick black line and the standard deviations with thin black lines. Substrate incubation time was 20 minutes.

Properties of PBST and RED buffer solution as diluents were compared with 16 serum samples in the Iran cohort and with two BuV1 VLP antigen concentrations: 10 ng and 20 ng per well. Median absorbance values for samples diluted in PBST were 0.106 and 0.158, with BuV1 VLP concentrations of 10 ng and 20 ng per well, respectively. Median absorbance values were very similar when diluted in RED buffer: 0.101 with BuV1 VLP concentration of 10 ng/well and 0.161 with 20 ng/well concentration. Results are presented in Figure 13. RED buffer was used as the diluent for screening the Iran serum sample cohort with BuV1 µ-capture IgM EIA.

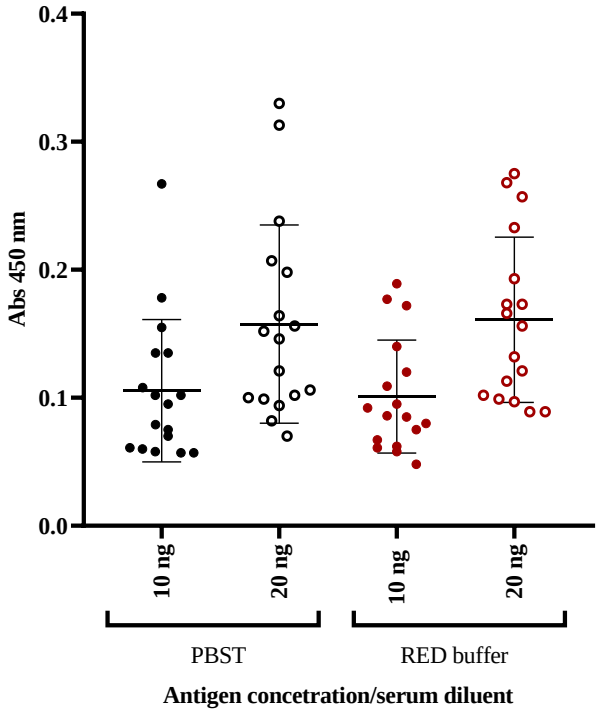


**Figure 13.** Two serum diluents, phosphate buffered saline solution with 0.05 % Tween 20 and RED buffer solution (Kaivogen), were compared in BuV1 µ-capture IgM EIA using two biotinylated BuV1 antigen concentrations: 10 ng and 20 ng/well. A total of 16 randomly selected serum samples in the Iran cohort were used for the assay. Substrate incubation time was 15 minutes. Absorbance values are grouped by diluent and the used antigen concentration. Results are presented with median (thick black line) and standard deviation (thin black line).

### *4.2.2. Screening the Iran serum sample cohort with the BuV1 µ-capture IgM EIA*

A total of 118 serum samples in the Iran cohort were analyzed with two concentrations of biotinylated BuV1 VLP antigens (10 ng and 20 ng per well) in the BuV1 µ-capture IgM EIA. With 10 ng of the biotinylated antigen in the well, the absorbance values varied from 0.034 to 0.744, median 0.126 and

with 20 ng per well concentration absorbance values fluctuated from 0.081 to 1.08, median 0.205. Results are presented in Figure 14. Samples N27 and N67 gave significantly high absorbance values in µ-capture IgM EIA, 0.744 and 0.518 with 10 ng per well concentration and 1.08 and 1.05 with 20 ng per well concentration, respectively. Also, Samples N18, N43, N44 and N101 gave relatively high absorbance values in the µ-capture IgM EIA with the 20 ng/well antigen concentration: 0.328, 0.463, 0.394 and 0.525, respectively. Samples N27, N67, N18, N43, N44 and N101 were considered putatively BuV1 IgM positive and were included in the competition IgM EIA panel. The well-characterized B19V-IgM positive and negative serum samples, used as technique and reagent controls for each assay, gave expected results in the B19V VP2 µ-capture IgM EIA.

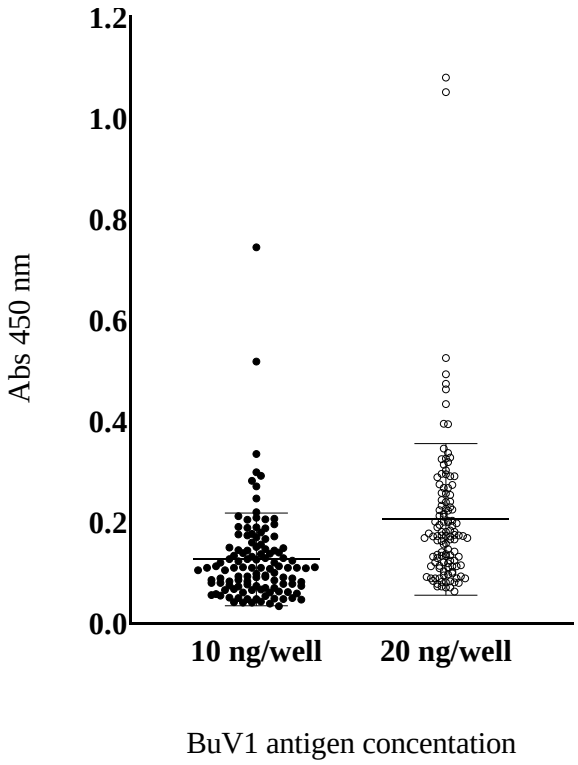


**Figure 14.** Samples in the Iran cohort (n=188) analyzed with BuV1 IgM µ-capture EIA with two antigen concentrations: 10 ng or 20 ng per well. Results are grouped by the antigen concentration and presented with the median absorbance value (thick black line) and standard deviation (thin black line).

With the 20 ng per well concentration of the biotinylated BuV1 VLPs, 40 samples gave absorbance values over 0.220. DNA was extracted from the 40 serum samples and analyzed with the Buv, TuV, CuV multiplex qPCR to detect possible viremia and to verify the BuV1 µ-capture IgM EIA results.

### *4.2.3. Results for the competition BuV1-3 and CuV µ-capture IgM EIA were ambiguous*

In order to evaluate the specificity of the VLP based IgM µ-capture EIA, two competition assays were done with six serum samples in the Iran cohort (N18, N27, N43, N44, N67 and N101). Each serum sample was subjected to no competition (corresponding to µ-capture IgM EIA) as well as to homologous and heterologous competition with BuV1-3 and CuV. Two concentrations were tested for the non-biotinylated (blocking) antigens in separate assays: 20 µg per ml in the first assay and 30 µg per ml in the second assay. All results are presented in Figure 15. The exhaustive competition and pre-incubation with homologous non-biotinylated antigen should block the binding sites from the common epitopes of the biotinylated VLP antigen, giving minimal residual absorbance values. The absorbance values in a single serum sample treated with no competition should be comparable between assays including the IgM µ-capture EIA results.

Based on the competition µ-capture IgM EIAs all six serum samples were interpreted as negative for BuV2 IgM antibodies, each sample gave absorbance value below 0.09. For the other analysed VLPs, the competition assays did not perform as expected. The absorbance values for single sample with no competition treatment in BuV3 or CuV competition IgM µ-capture EIA were not comparable when the assays were repeated (Figure 15). Moreover, in the case of the BuV1 EIAs, the absorbance values for individual sample were comparable neither in the no competition treatment in the competition IgM µ-capture EIAs nor in the µ-capture EIA (Table 5, Figure 15.). For example, Sample N67 gave absorbance values of 1.051 and 0.518 in the BuV1 µ-capture IgM EIA with 10 ng and 20 ng biotinylated VLPs per well, respectively. However, the absorbance levels were 0.271 and 0.328 with no competition treatment in the BuV1 competition µ-capture IgM EIA. Similar incoherence in absorbance values can be detected also for the other five serum samples (N18, N27, N43, N44 and N101) when measured for BuV1 VLP antibodies. In the case of CuV µ-capture IgM EIA competition panels, the absorbance values were blocked neither by the homologous nor the heterologous competition in most cases, indicating non-specific reactivity. For example, Sample N18 gave absorbance values of 0.603 with no competition, 0.534 with homologous competition and 0.493 with heterologous competition (30 µg well of each non-biotinylated antigen). Based on these results, several components of the µ-capture IgM EIA were studied to track down the reason behind the incoherent and non-specific results.

**Table 5.** Examples of absorbance values in the BuV1 µ-capture IgM EIA and in the in the no competition treatment in the competition BuV1 µ-capture IgM EIA. Assay A: The BuV1 µ-capture IgM EIA for all samples in the Iran serum sample cohort, with two BuV1 antigen concentrations: 10 ng and 20 ng/well, B. The no competition treatment in the competition BuV1 µ-capture IgM EIA C. The no competition treatment in the second competition BuV1 µ-capture IgM. The absorbance values from the no competition treated wells in the competition µ-capture IgM EIA should be comparable with the results in BuV1 µ-capture IgM EIA.

| Biotinylated antigen in the well | BuV1 10 ng/well | | | BuV1 20 ng/well |
|---|---|---|---|---|
| Sample ID | Absorbance value (450 nm) | | | |
| Type of assay | A. | B. | C. | A. |
| N27 | 0.744 | 0.244 | 0.110 | 1.080 |
| N43 | 0.299 | 0.244 | 0.134 | 0.463 |
| N44 | 0.271 | 0.576 | 0.129 | 0.394 |
| N67 | 0.518 | 0.271 | 0.328 | 1.051 |
| N18 | 0.188 | 0.366 | 0.112 | 0.328 |
| N101 | 0.335 | 0.147 | 0.123 | 0.525 |

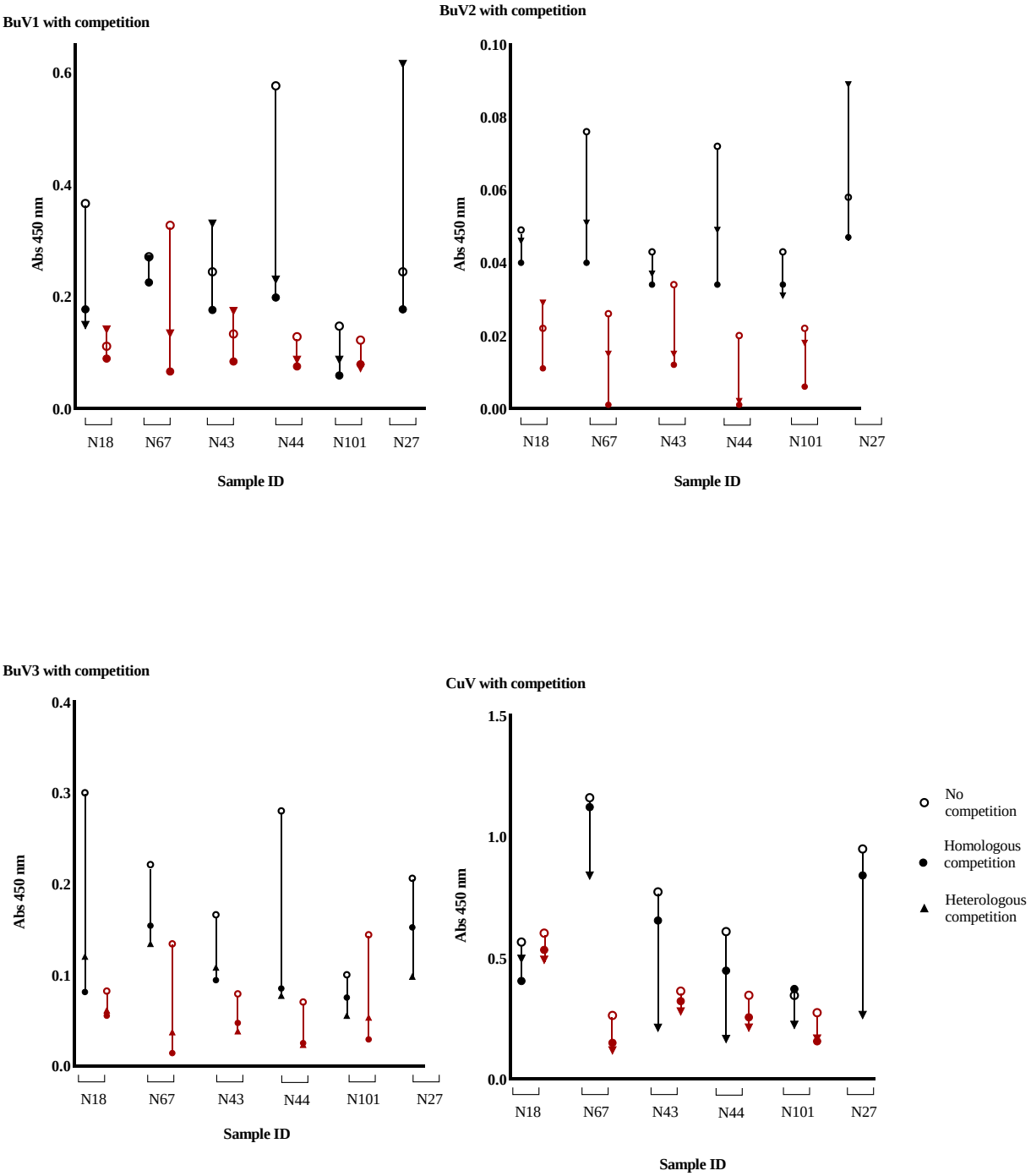


**Figure 15.** Six serum samples in the Iran cohort analyzed with the BuV1-3 and CuV competition µ-capture IgM EIAs. From top left to the bottom right: BuV1, BuV2, BuV3 and CuV IgM EIA, with no competition (circle with no fill), homologous competition (circle with fill) and heterologous competition (triangle). Symbols marked with black represent the competition assay done with 20 µg/ml of non-biotinylated antigen and symbols marked with red the assay with 30 µg/ml non-biotinylated antigen.

### *4.2.4. BuV, TuV or CuV DNA was not found in the selected 40 serum samples in the Iran cohort by multiplex qPCR*

All serum samples in the Iran cohort, which gave an absorbance value of 0.220 or higher in the BuV1 µ-capture IgM EIA (n=40), were analyzed with the BuV, TuV, CuV multiplex qPCR, to study possible viremia and verify the EIA results. The DNA from the serum samples was extracted with the phenol-chloroform extraction method. Replicates of each sample were analyzed in separate qPCR assays with 10 extraction controls and 6 negative controls in each. In the first multiplex qPCR assay 5 out of 40 samples were positive for CuV DNA and none for BuV or TuV DNA. In the second assay 3 out of the 40 analyzed samples were positive for CuV DNA and none for BuV or TuV DNA. In addition, one extraction control was positive for CuV DNA. Only one sample was positive in both qPCR runs. All samples, and the extraction control, which gave a positive result in the multiplex qPCR were analyzed in replicates with CuV singleplex qPCR with 6 negative controls. None were positive. All serum samples were considered negative for BuV, CuV and TuV DNA, which indicates that the putatively positive results in the BuV1 µ-capture IgM EIAs, were false positives.

### *4.2.5. Troubleshooting the µ-capture IgM EIA*

Due to the incoherent results in the competition µ-capture IgM EIA (Figure 15, Table 5.), the assay and assay performance was investigated. All laboratory notes were revised, to detect any mistake in calculations or in execution of the assays. Nothing that could explain the results was found. Next, the antiserum-coated strips stored for 1 day, 10 days, 3 months and 1 year and a new and old aliquot of the streptavidin conjugate were studied. The strips and the streptavidin conjugate were tested with the B19V µ-capture IgM EIA (Maple *et al.*, 2014) using well-characterized B19V-IgM positive and negative serum samples and with BuV1 µ-capture IgM EIA using the Sample N30 from the Iran serum sample cohort. There was no significant difference in absorbance values regardless of whether the sample was treated with the old or the new aliquot of streptavidin conjugate or which strip was used (Figure 16.). For example, the absorbance values for the known B19V IgM-positive serum varied in B19V IgM EIA from 2.22 to 1.93 with different antiserum-coated strips (the cutoff values for B19V borderline and -IgM positivity is 0.171-0.220, respectively). The well-characterized B19V-IgM negative serum sample was negative in all the tests, the median absorbance values varied from 0.03 to 0.02 (the cutoff value for a negative B19 IgM is < 0.171). Absorbance values for Sample N30 varied from 0.09 to 0.06 with the BuV1 µ-capture IgM EIA and was considered negative based on

these tests. It was evaluated that neither the strips nor the used streptavidin conjugate was the reason behind the incoherent results in the competition µ-capture IgM EIA.

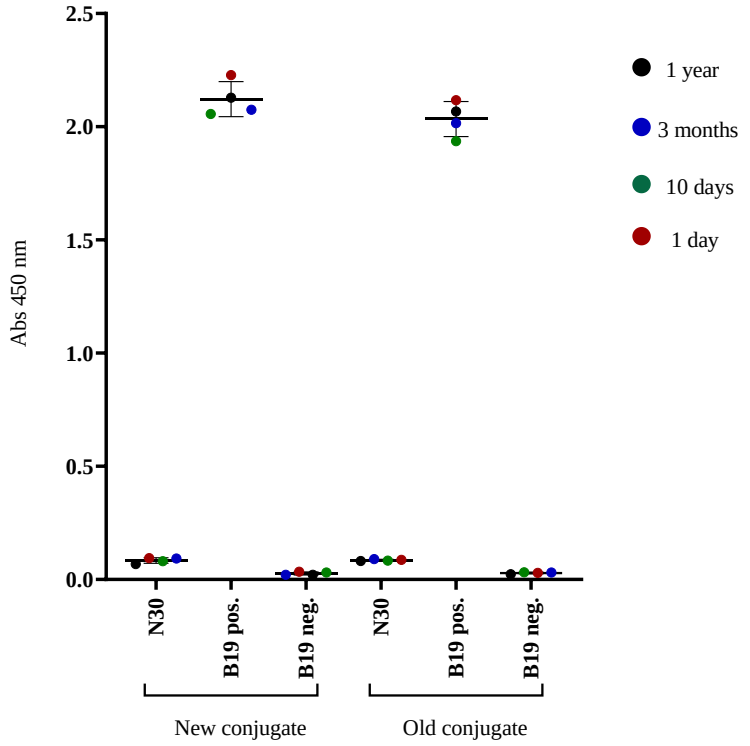


**Figure 16.** Testing the antiserum-coated strips after 1 day, 10 days, 3 months and 1 year of storage as well as a new and old aliquot of the streptavidin conjugate. The results are grouped on the x-axis by the used streptavidin aliquot. The colors of the dots represent the storage time of the strips: 1 day (red), 10 days (green), 3 months (blue) and 1year (black). Absorbance value measured at 450 nm is on the y-axis.

### *4.2.6. The CuV VLP production and testing of the new VLPs in CuV IgG and IgM EIA*

In orded to study whether the purity, storage or the used VLP batch effected the performance of the µ-capture IgM EIA, new CuV VLPs were produced. CuV VLPs were chosen to be produced due to the incoherent results in the competition CuV µ-capture IgM EIAs and our stock were becoming scarce. The prepared batches of biotinylated and non-biotinylated CuV VLPs were purified two times by ultracentrifugation to remove all possible impurities. The correct size of the produced CuV VLPs was verified by SDS-PAGE (Figure 17.). The correct size for the CuV VP2 VLP is ~65 kilodaltons (kDa) (Väisänen *et al.*, 2018). The CuV VLP production was successful and yielded two batches, which were tested in CuV IgG EIA (Väisänen *et al.*, 2016) and in CuV µ-capture IgM EIA.

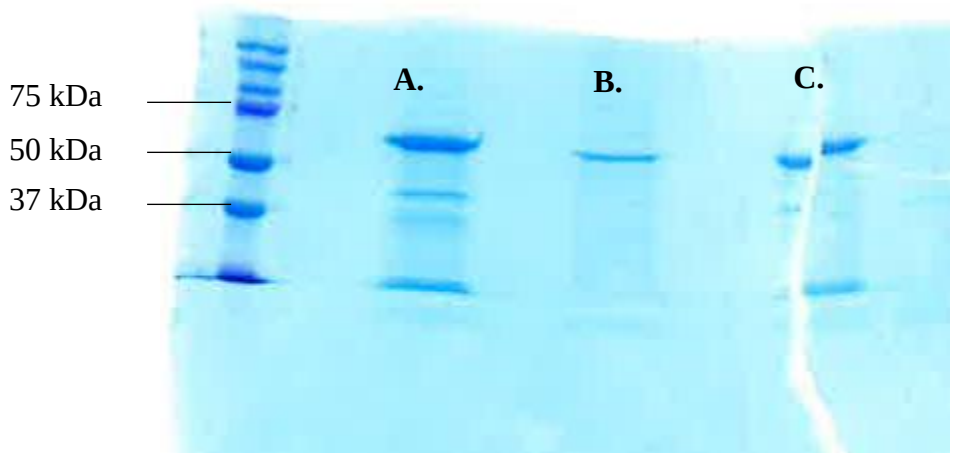


**Figure 17.** SDS-PAGE gel of the produced CuV VLPS after 2x ultracentrifugation. From left to right: Precision Plus Protein™ Dual Color Standard (Bio-Rad), A: the old batch of the CuV VLPs, B. batch no. 1 of the new CuV VLPs and C. new batch no.2 of the new CuV VLPs. The correct size for the CuV VP2 VLP is ~65 kDa.

The performance of the produced biotinylated and non-biotinylated CuV VLPs was tested in CuV IgG EIA with no competition using biotinylated antigen concentrations of 80 ng and 160 ng per well. The CuV VLPs were tested in a competition assay with homologous and heterologous competition using non-biotinylated CuV and BuV2 VLPs, respectively (Väisänen *et al.*, 2016). Serum samples GoSe and VaPa, which are known to be CuV positive and negative, respectively, were used to test the CuV VLPs. In addition, Sample M60, which is known to be CuV IgG cross-reactive and BuV1-3 IgG-positive, was included in the test panels. The CuV VLPs performed as expected (Figure 18.). For example, Sample GoSe gave absorbance values from 4.06 to 3.74 in CuV IgG EIA without competition, VLP concentrations 80 ng and 160 ng/well, respectively. When Sample GoSe was assigned to homologous competition with non-biotinylated CuV VLPs the absorbance value was blocked to 0.10.

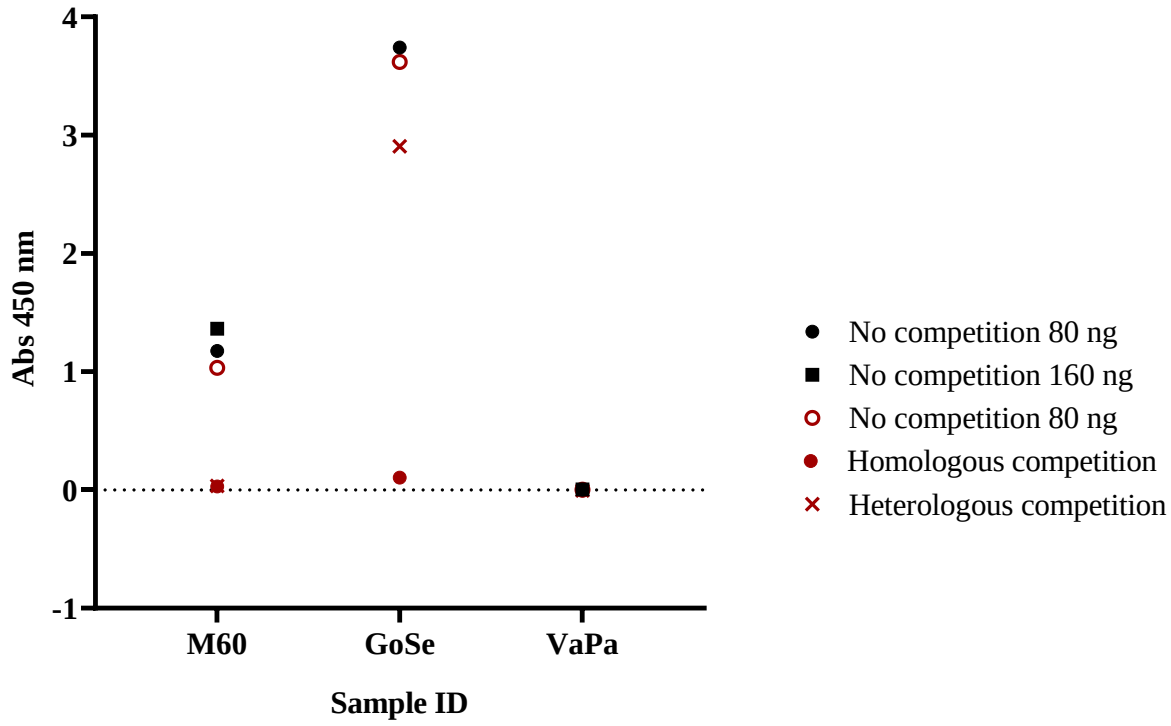


**Figure 18:** The new batch of biotinylated and non-biotinylated CuV VLPs in CuV IgG EIA. Absorbance was measured at 450 nm (y-axis) and the results are grouped by the sample. The black color marks the CuV IgG EIA with no competition. The red color marks the CuV IgG competition EIA panel.

To test whether the ambiguous results in the CuV µ-capture IgM EIA with competition were related to the batch of CuV VLPs used, the new batch of CuV VLPs were tested in CuV µ-capture IgM EIA with competition, homologous and heterologous (BuV1-3) competition treatments. The competition assay was performed using six serum samples from the Iran cohort: N18, N27, N43, N44, N67 and N101. The samples gave a mean absorbance value of 0.192 with the new batch of CuV VLPs in the no competition treatment (Figure 19.). The pre-incubation with the new batch of non-biotinylated CuV VLPs reduced the absorbance value by approximately 40 % in homologous competition µ-capture IgM EIA. Overall, the new batch of CuV VLPs gave significantly lower absorbance values when compared to the absorbance values gained with the old batch of CuV VLPs (Figure 15.).

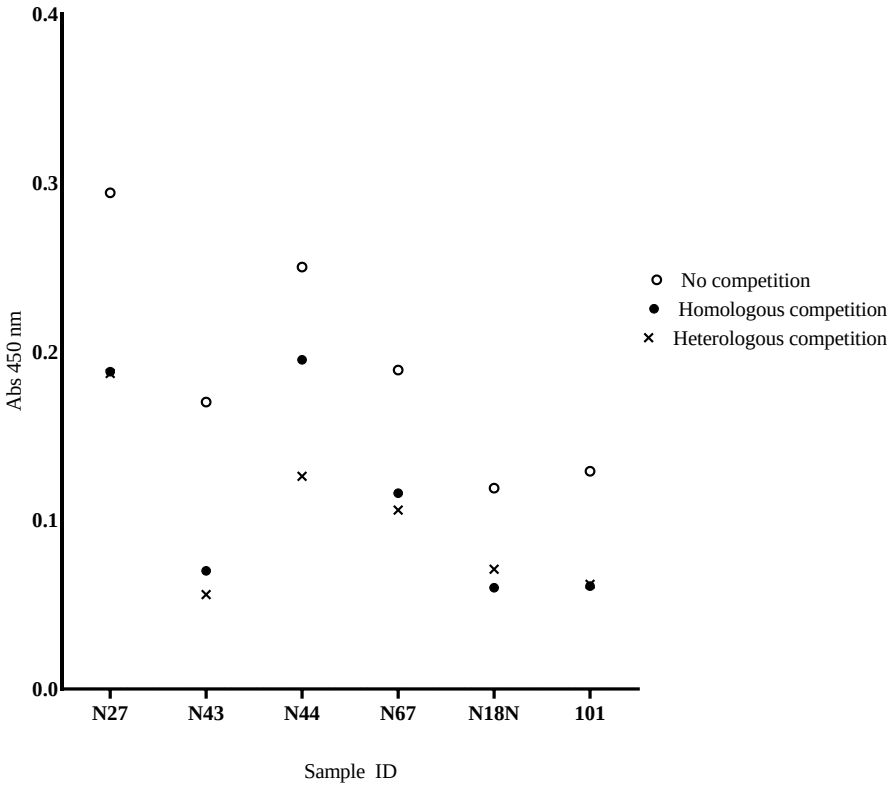


**Figure 19.** The new batch of CuV VLPs in IgM μ-capture EIA tested with six samples in the Iran cohort. The circle with no fill marks for the no competition treatment, circle with fill mars for the homologous competition treatment and the cross marks for heterologous competition with BuV1-3. The assay was performed with 10 ng per well of biotinylated antigen and 30 μg/ml of the non-biotinylated antigen

## 5. DISCUSSION

Several new viruses have been identified during the last few decades due to the developments in the field of next generation sequencing. Parvoviruses BuV, TuV and CuV were discovered in the last seven years in human samples (Phan *et al*., 2012; Phan *et al.*, 2014; Phan *et al.*, 2016). BuV DNA has been found in stool samples and it is associated with gastrointestinal illnesses (Phan *et al.*, 2012; Väisänen *et al.*, 2014, 2016; Yahiro *et al.*, 2014; A. Altay *et al.*, 2015; Chieochansin, 2015; Ayouni *et al.*, 2016). CuV is suggested to have a connection to skin cancers and CuV DNA has been found in skin biopsies of patients with CTCL or melanoma (Phan *et al.*, 2016; Mollerup *et al.*, 2017; Kreuter *et al.*, 2018, Väisänen *et al.*, 2018). IgG EIA has been developed for BuV1-3, CuV and TuV and striking differences in geographical distribution for BuV has been identified (Väisänen *et al.*, 2016, 2018). There were two main aims for this thesis work: to screen three stool sample cohorts with in-house BuV, TuV, CuV multiplex qPCR and to develop an IgM EIA for human protoparvoviruses.

### *5.1. TuV and CuV were found in stool since the discovery of the viruses*

This is the first study to identify TuV DNA, since its discovery in 2014 in feces of 18-months-old girl, with unexplained diarrhea (Phan *et al.*, 2014). After the discovery, TuV IgG has been reported in two subjects in Finland, but no TuV DNA has been searched nor found in human stool (Väisänen *et al.*, 2016, 2018). In 2016, a sequence resembling TuV DNA was found in seal furs in South America (Kluge *et al.*, 2016), but there is no other mention of the virus DNA in scientific publications since 2014. In this study, TuV DNA was found in 0.25 % of the analyzed stool samples (n=407). The TuV DNA-positive amplicon had a total of 6 mismatches, when compared to the TuV plasmid standard, thus contamination from the plasmid standard can be ruled out. The TuV DNA-positive sample was from the HUSLAB b cohort, but no diarrhea causing bacteria had been found from the sample by HUSLAB. The patient had been travelling in Turkey and Jamaica, but no additional information was available from this patient.

CuV DNA was found in 2.9 % of the stool samples (n=407) by qPCR in this study and the results were verified by sequencing. Before this, CuV DNA has been described in skin biopsies of CTCL, organ transplant and melanoma patients (Phan *et al.*, 2016; Väisänen *et al.*, 2019; Mollerup *et al.*, 2017). CuV is one of the newest members of the *Parvoviridae* family and due to its possible link to cancer it has quickly become the most studied emerging parvovirus. During 2018 six papers (pubmed.gov) addressing CuV were published.

In the case of BuV, virus DNA was found in one stool sample (0.2 %) in the Malawi cohort. Since its discovery in 2012 (Phan *et al.*, 2012) BuV has been repeatedly found by PCR-based methods in stool samples and the virus has been linked to gastrointestinal illnesses. BuV DNA was also recently found in urban streams of the capital of Ecuador by metagenomics (Guerrero-Latorre *et al.*, 2018). Overall, the reported viral loads as well as the reported prevalence of detected BuV DNA has been relatively low with median prevalence of 1,8 % (Phan *et al.*, 2012, Altay *et al*., 2015; Chieochansin *et al*., 2015; Smits *et al*. 2014; Väisänen *et al*.2014, 2016; Yahiro *et al*. 2014).

### *5.1.1. Primer cross reactivity in the multiplex qPCR*

Primer-cross reactivity was observed during the BuV, TuV, CuV multiplex qPCR analyses. Samples 54 and 13FV10 gave positive qPCR signals for CuV and TuV, respectively, but were deemed false positives based on the sequence analysis. Sample 13FV10 derived amplicon was identified as *Alistipes shahii* bacteria and, interestingly, the amplicon from Sample 54 was identified as BuV (2 or 3) based on sequence and BLAST analysis.

The BuV, TuV, CuV multiplex qPCR reaction mixture has a total of 6 primers and 3 probes. Despite the careful assay design, the possibility of amplifying a non-target nucleotide sequence exists. In this study, from a total of 407 qPCR analyzed stool samples, 0.49 % gave a false positive signal, which results in assay specificity of 99.51 %. Further optimizing of the assay might be possible to increase specificity. With that being said, the BuV, CuV, TuV multiplex qPCR assay is highly sensitive, the reported limit of detection (LOD) of the assay is at ≤ 10 copies/µL (Väisänen *et al.*, 2018), but as was seen in this study the assay can detect copy numbers as low as 1 copy/µL. In the case of BuV, TuV, and CuV the detected viral loads are normally extremely low and the assay sensitivity might be more important than absolute specificity.

## 5.2. The protoparvovirus IgM EIA requires more optimization

In addition to qPCR screening of the stool sample cohorts, the other aim of this thesis work was to develop a human protoparvovirus µ-capture IgM EIA using BuV1 as an example. Several steps were taken to optimize and later to troubleshoot the assay and its components. The protoparvovirus µ-capture IgM EIA development was not finalized in this study. The assay requires further optimization, before it can be used for sample screening. However, this study offers a good base for future assay development. Acquiring a positive control, for example immunized rabbit sera or BuV1-3 or CuV IgM-positive serum sample from a patient, is crucial for further assay design. In addition to that, the effect of VLP-batch variability and storage of the VLPs on the IgM EIA should be more carefully

studied. The used biotinylated BuV1 VLPs in this study had been stored for approximately two years and thawed several times, this can damage the structure of the VLPs. It could be worth investigating the storage conditions, how the storage affects the VLPs and could the storage and freezing solution be improved. Adding trehalose or sucrose to the mix can improve the stability of the capsids during long-time storage (Wang *et al.*, 2017; Lan *et al.*, 2018). Based on this study all samples in the Iran serum sample cohort (n=118) were identified IgM-negative for BuV1.

### 5.3.Conclusions and future prospects

Tools to develop assays able to detect viral DNA or specific antibodies are in the core, when studying emerging viruses, the distribution, what kind symptoms the viruses cause and what kind of risk they pose to human health. BuV has been detected in Europe, Africa and Asia, and the BuV DNA-positive fecal sample from Malawi presented in this study further on supports the theory that the virus has spread globally. In this study, CuV DNA was found from all the stool sample cohorts. This supports the hypothesis of CuV having a possible role in gastrointestinal illnesses (Phan *et al.*, 2016; Väisänen *et al.*, 2017). Since CuV DNA has now been found from skin biopsies as well as from stool samples, it can speculated, whether the virus can cause systemic infections. Therefore, CuV studies should not be limited to cancer patients only. TuV findings have been scarce and this study is the first to identify TuV DNA since the discovery of the virus. The detected viral load was low and can be, in theory, derived from a dietary or other contamination. More research on TuV is needed to verify its role as a human virus. TuV is phylogenetically very closely related to rodent viruses and it would be interesting to screen animal derived samples using the BuV, TuV, CuV multiplex qPCR.

Catching an acute BuV, CuV or TuV infection is at the heart of the emerging human protoparvovirus research. Since it is now known that there is differences in BuV IgG distribution globally (high seroprevalence in Middle East and Kenya) (Väisänen *et al.*, 2018), the search of acute infections can be pinpointed to a certain geographical area. The development of a sensitive and specific protoparvovirus IgM EIA will be continued. When successful, the IgM serology can be combined with the highly sensitive BuV, TuV, CuV qPCR assay in the future. The combination of these assays will shed more light on human protoparvovirus pathogenity, distribution, symptoms and possibly transmission.

## 6. ACKNOWLEDGEMENTS

I want to thank my supervisor docent Maria Söderlund-Venermo for this thesis subject and critical reading of my work. I want to thank my supervisor docent Ausra Domanska and Professor Sarah Butcher for guidance and for extremely valuable feedback. I want to thank Elina Väisänen and Lea Hedman for all the help regarding lab work and execution of the assays. I want to thank Man Xu and Yilin Wang for the unmeasurable amount of help and support they have given me. I want to thank my family for believing in me and for not asking too many questions of how this project is coming along.

# 7. REFERENCES


Allander, T., Tammi, M. T., Eriksson, M., Bjerkner, A., Tiveljung-lindell, A. & Andersson B. (2005). Cloning of a human parvovirus by molecular screening of respiratory tract samples. *PNAS* 102, 12891-12896

Allander, T., Andreasson, K., Gupta, S., Bjerkner, A., Bogdanovic, G., Persson, M. A. A., & Dalianis, T., (2007) Identification of a third human polyomavirus. *Journal of Virology* 81, 4130–4136.

Allander, T., Jartti, T., Gupta, S., Niesters, H. G., Lehtinen, P., Osterback R., Vuorinen T., Waris M., Bjerkner A., Tiveljung-Lindell A., van den Hoogen, B. G., Hyypiä T. & Ruuskanen O. (2007) Human bocavirus and acute wheezing in children. *Clinical Infectious Diseases* 44, 904–910.

Altay, A., Yahiro, T., Bozdayi, G., Matsumoto, T., Sahin, F., Ozkan, S., Nishizono A., Söderlund Venermo M. & Ahmed, K. (2015) Bufavirus genotype 3 in Turkish children with severe diarrhoea. *Clinical Microbiology and Infection* 21, 965.e1-965

Arthur, J. L., Higgins, G. D., Davidson, G. P., Givney, R. C., & Ratcliff, M. R. (2009) A novel bocavirus associated with acute gastroenteritis in Australian children. *PLOS Pathogens* 5, e1000391

Astell, C. R., Chow, M. B. and Ward, D. C. (1985) Sequence analysis of the termini of virion and replicative forms of minute virus of mice dna suggests a modified rolling hairpin model for autonomous parvovirus DNA replication. *Journal of Virology* 54, 171–177.

Atchison, R. W., Casto, B. C. & Hammon, W. McD. (1965). Adenovirus-associated defective virus particles. *Science* 13, 754-755.

Ayouni, S., Estinney, M., Hammami, S., Neji Guediche, M., Pothier, P., Auoni, M., Belliot, G. & de Rougemont A. (2016). Cosavirus, salivirus and bufavirus in diarrheal Tunisian infants, *PLoS ONE* 11, 1–11.

Berns, K., I. & Parrish, C., R. (2013). Chapter 57: Parvoviridae In: Knipe, D. M. & Howley, P. (Editors-in-Chief). Field's Virology 6th edition, Wolters Kluwer, Lippincott, Williams & Wilkins

Bexfield, N., & Kellam, P. (2011). Metagenomics and the molecular identification of novel viruses. *The Veterinary Journal* 190, 191–198.

Bibby, K. (2013) Metagenomic identification of viral pathogens. *Trends in Biotechnology* 31, 275 279.

Bleker, S., Sonntag, F. and Kleinschmidt, J. A. (2005). Mutational analysis of narrow pores at the fivefold symmetry axes of adeno-associated virus type 2 capsids reveals a dual role in genome packaging and activation of phospholipase A2 activity. *Journal of Virology* 79, 2528–2540.

Bowles, D. E., Rabinowitz, J. E. & Samulski R. J. (2006). The genus Dependovirus. In: Kerr, T., Cotmore, S. F., Bloom, M. E., Linden, R. M. & Parrish, C. R. (Eds.). Parvoviruses, Hodder Arnold Publication, pp. 15-23

Breitbart, M., Salamon, P., Andresen, B., Mahaffy, J. M., Segall, A. M., Mead, D., Azam F. & Rohwer, F. (2002). Genomic analysis of uncultured marine viral communities. *PNAS* 99, 14250-14255.

Briese, T., Paweska, J. T., McMullan, L. K., Hutchison, S. K., Street, C., Palacios, G., Khristova, M. L., Weyer, J., Swanepoel, R., Egholm, M., Nichol, S. T. & Lipkin, I. (2009), Genetic detection and characterization of lujo virus, a new hemorrhagic fever–associated arenavirus from Southern Africa. *PLOS Pathogens* 5, e1000455.

Brown, T, Ritchie, L, Clewley, J, & Reid, T. (1984). Intrauterine parvovirus infection associated with hydrops fetalis. *The Lancet* 2, 1033– 1034.

Bär, S., Rommelaere, J. and Nüesch, J. P. F. (2013). Vesicular transport of progeny parvovirus particles through er and golgi regulates maturation and cytolysis, *PLOS Pathogens* 9, e1003605

Chen, T., Hedman, L., Mattila, P. S., Jartti, T., Ruuskanen, O., Söderlund-Venermo, M., & Hedman, K. (2011). Serological evidence of Merkel cell polyomavirus primary infections in childhood. *Journal of Clinical Virology* 50, 125–129.

Deiss, V., Tratschin, J.D., Weitz, M. & Siegl, G. 1990. Cloning of the human parvovirus-B19 genome and structural-analysis of its palindromic termini. *Virology* 175, 247-254.

Chieochansin, T., Vutithanachot, V., Theamboonlers, A., & Poovorawan, Y. (2015). Bufavirus in fecal specimens of patients with and without diarrhea in Thailand. *Archives of Virology* 160, 1781–1784.

Chung, Y., Jun, H. S., Son, M., & Bao, M. (2014). Cellular and molecular mechanism for Kilham rat virus-induced autoimmune diabetes in DR-BB rats. *The Journal of Immunology* 165, 2866-2876.

Cotmore, S. F. and Tattersall, P. (1986). Organization of nonstructural genes of the autonomous parvovirus minute virus of mice., *Journal of virology* 58, 724–32.

Cotmore, S. F., & Tattersall, P. (2006). Structure and organization of the viral genome. In: Kerr, T., Cotmore, S. F., Bloom, M. E., Linden, R. M. & Parrish, C. R. (Eds.). Parvoviruses, Hodder Arnold Publication, pp. 74-94

Cotmore, S. F., & Tattersall, P. (2007). Parvoviral host range and cell entry mechanisms. *Advances in Virus Research* 70, 183–232.

Cotmore, S. F., Agbandje-McKenna, M., Chiorini, J. A., Mukha, D. V., Pintel, D. J., Qiu, J., Söderlun-Venermo, M., Tattersall, P., Tijssen, P., Gatherer, D. & Davison, A. J. (2014). The family Parvoviridae. *Archives of Virology* 159, 1239–1247.

Cotmore, S. F., & Tattersall, P. (2014). Parvoviruses: small does not mean simple. *Annual Review of Virology* 1, 517–537.

Cossart, Y. E., Field, A. M., Cant, B. & Widdows, C. (1975). Parvovirus-like particles in human sera., *Lancet* 1 72-73

Deng, X., Yan, Z., Cheng, F., Engelhardt, J. F., & Qiu, J. (2016). Replication of an autonomous human parvovirus in non-dividing human airway epithelium is facilitated through the dna damage and repair pathways. *PLoS Pathogens* 12, 1–25.

Ellerman, K. E., Richards, C. A., Guberski, D. L., Shek, W. R., & Like, A. A. (1996.). Kilham rat virus triggers T-cell-dependent autoimmune diabetes in multiple strains of rat, *Diabetes* 45, 557–562.

Farr, G. A., Zhang, L. -g., & Tattersall, P. (2005). Parvoviral virions deploy a capsid-tethered lipolytic enzyme to breach the endosomal membrane during cell entry. *Proceedings of the National Academy of Sciences* 102, 17148–17153.

Finkbeiner, S. R., Li, Y., Ruone, S., Conrardy, C., jonoricus, N., Toney, D.,Virgin H., Anderson L. J., Vinje J., Wang D. & Tong, S. (2009). Identification of a novel astrovirus (astrovirus VA1) associated with an outbreak of acute gastroenteritis, *Journal of virology* 83, 10836–10839.

Gaynor, A. M., Nissen, M. D., Whiley, D. M., Mackay, I. M., Lambert, S. B., Wu, G., Brennan D. C., Storch G. A., Sloots T. P. & Wang, D. (2007). Identification of a novel polyomavirus from patients with acute respiratory tract infections, *PLOS Pathogens* 3, 0595-0604

Guerrero-Latorre, L., Romero, B., Bonifaz, E., Timoneda, N., Rusinol, M., Girones., Rios-Touma, B. (2018). Quito's virome: Metagenomic analysis of viral diversity in urban streams of Ecuador's capital city, *Science of the Total Environment* 645, 1334–1343.

Hristov, G., Krämer, M., Li, J., El-Andaloussi, N., Mora, R., Daeffler, L., Zentgraf, H., Rommelaere, J. & Marchini, A. (2010). Through its nonstructural protein ns1, parvovirus h-1 induces apoptosis via accumulation of reactive oxygen species. *Journal of Virology* 84, 5909–5922.

Huang, Q. Deng, X., yan, Z., Cheng, F., Luo, Y., Shen, W., Lei-Butters, D. C. M, Chen, A. Y., Li, Y., Tang, L., Söderlund-Venermo, M., Engelhardt, J. F. & Qiu, J. (2012). Establishment of a reverse genetics system for studying human bocavirus in human airway epithelia, *PLoS Pathogens* 8, e1002899

Ilyas, M., Mietzsch, M., Kailasan, S., Väisänen, E., Luo, M., Chipman, P., Smith, J. K., Kurian, J., Sousa, D., McKenna, R., Söderlund-Venermo, M. & Agbandje-Mckenna, M. (2018). Atomic resolution structures of human bufaviruses determined by cryo-electron microscopy. *Viruses*, 10, 22

Jones, M. S., Kapoor, A., Lukashov, V. V, Simmonds, P., Hecht, F., & Delwart, E. (2005). New DNA viruses identified in patients with acute viral infection syndrome, *Journal of Virology*, 79, 8230–8236.

Kantola, K., Hedman, L., Allander, T., Jartti, T., Lehtinen, P., Ruuskanen, O., Hedman K. & Soderlund-Venermo, M. (2008). Serodiagnosis of human bocavirus infection. *Clinical Infectious Diseases*, 46, 540–546.

Kantola, K., Hedman, L., Arthur, J., Alibeto, A., Delwart, E., Jartti, T., Ruuskanen, O., Hedman K. & Soderlund-Venermo, M. (2011). Seroepidemiology of Human Bocaviruses 1-4, *Journal of Infectious diseases,* 204, 1403–1412.

Kantola, K., Hedman, L., Tanner, L., Mäkinen, M., Partanen, J., Sadeghi, M., Veijola, R., Knip, M., Ilonen, J., Hyöty, H., Toppari, K., Simell, O., Hedman, K & Söderlund-Venermo, M. (2015). B-cell responses to human bocaviruses 1–4: new insights from a childhood follow-up study. *PLOS One* 10, e0139096

Kapoor, A., Simmonds, P., Slikas, B., Li, L., Bodhidatta, L., Sethabutr, O., Triki H., Bahri O., Oderinde B. S., Baba M. M., Bukbuk, D. N., Besser J., Bartkus, J.& Delwart E. (2009). A new bocavirus species in human stool. *The Journal of Infectious Diseases* 15, 196-200

Kapoor, A., Simmonds, P., Slikas, E., Li, L., Bodhidatta, L., Sethabutr, O., Triki H., Bahri O., Oderinde B. S., Baba M. M., Bukbuk, D. N., Besser J., Bartkus, J.& Delwart E. (2010). Human bocaviruses are highly diverse, dispersed, recombination prone, and prevalent in enteric infections. *The Journal of Infectious Diseases* 201, 1633–1643.

Kilham, L & Olivier, L. (1959) A latent virus of rats isolated in tissue culture. *Virology* 7, 428 – 437.

Kluge, M., Campos, F. S., Tavares, M., de Amorim, D. B., Valdez, F. P., Giongo, A. Roehe P. M. & Franco, A. C. (2016). Metagenomic survey of viral diversity obtained from feces of Subantarctic and South American fur seals. *PloS One* 11, e0151921.

Lan, N. T., Kim, H. J., Han, H. J., Lee, D. C., Kang, B. K., Han, S. Y., Moon H. &Kim, H. J. (2018). Stability of virus-like particles of red-spotted grouper nervous necrosis virus in the aqueous state, and the vaccine potential of lyophilized particles. *Biologicals:Journal of the International Association of Biological Standardization* 51, 25–31.

Li, L., Cotmore, S. F., & Tattersall, P. (2013). Parvoviral left-end hairpin ears are essential during infection for establishing a functional intranuclear transcription template and for efficient progeny genome encapsidation. *Journal of Virology* 87, 10501–10514.

Li, Y. Yan, Z., Luo, Y., Xu, J., Cheng, F., Li, Y., Engelhardt, E. & Qiu, J. (2013). In vitro modeling of human bocavirus 1 infection of polarized primary human airway epithelia. *Journal of Virology* 87, 4097–4102.

Lombardo, E., Ramirez, J. C., Agbendje-McKenna, M. & Almendral, J. M. (2002) A beta-stranded motif drives capsid protein oligomers of the parvovirus minute virus of mice into the nucleus for viral assembly. *Journal of Virology* 74, 3804–3814.

Luo, Y. and Qiu, J. (2015). Human parvovirus B19: A mechanistic overview of infection and DNA replication. *Future Virology* 10, 155–167.

Lou, S., Luo, Y., Cheng, F., Huang, Q., Shen, W., Kleiboeker, S., Tisdale, J. F., Liu, Z. & Qiu, J. (2012) Human parvovirus B19 DNA replication induces a dna damage response that is dispensable for cell cycle arrest at phase G2/M, *Journal of Virology* 86, 10748–10758.

Maggi, F., Andreoli, E., Pifferi, M., Meschi, S., Rocchi, J., & Bendinelli, M. (2007). Human bocavirus in Italian patients with respiratory diseases. *Journal of Clinical Virology* 38, 321–325.

Maple, P. A. C., Hedman, L., Dhanilall, P., Kantola, K., Nurmi, V., Söderlund-Venermo, M., Brown K. E. & Hedman, K. (2014). Identification of past and recent parvovirus B19 infection in immunocompetent individuals by quantitative PCR and enzyme immunoassays: A dual-laboratory study. *Journal of Clinical Microbiology* 52, 947–956.

Maroto, B., Valle, N., Saffrich, R. & Almendral, J. M. (2004). Nuclear export of the nonenveloped parvovirus virion is directed by an unordered protein signal exposed on the capsid surface, *Journal of Virology* 78, 10685–10694.

Matthews, P. C., Malik, A., Simmons, R., Sharp, C., Simmonds, P., & Klenerman, P. (2014). PARV4: An emerging tetraparvovirus, *PLOS Pathogens* 10, 3–6.

Moffat S., Yeagashi N., Tada K., Tanaka N., Sugamura K., 1998: Human parvovirus B19 nonstructural (NS1) protein induces apoptosis in erythroid lineage cells, *Journal of Virology* 74, 3018–3028

Mollerup, S., Fridholm, H., Vinner, L., Kjartansdóttir, K. R., Friis-Nielsen, J., Asplund, M., Herrera J. A. R., Steiniche T., Mourier T., Brunak, S., Willerslev E., Izarzugaza, J. M. G., jhanser A. J. & Nielsen, L. P. (2017). Cutavirus in cutaneous malignant melanoma. *Emerging Infectious Diseases* 23, 363–365.

Mullis, K. (1990) The unusual origin of the polymerase chain reaction. *Scientific American*, April, 56-65.

Mukha, D. V., Chumachenko, A. G. Dykstra, M. J., Kurtti, T. J. &Schal C. (2006). Characterization of a new densovirus infecting the German cockroach, Blattella germanica, *Journal of General Virology* 87, 1567–1575.

Op De Beeck, A., & Caillet-Fauquet, P. (1997). The NS1 protein of the autonomous parvovirus minute virus of mice blocks cellular DNA replication: a consequence of lesions to the chromatin? *Journal of Virology* 71, 5323–5329.

Parrish, C., R. (2006). Autonomous parvovirus variation and evolution. In: Kerr, T., Cotmore, S. F., Bloom, M. E., Linden, R. M. & Parrish, C. R. (Eds.). Parvoviruses, Hodder Arnold Publication, pp. 47-53

Parrish, C., R. & Hueffer, K. (2006). Parvovirus host range, cell tropism and evolution – studies of canine and feline parvoviruses, minute virus of mice, porcine parvovirus, and Aleutian mink disease virus. In: Kerr, T., Cotmore, S. F., Bloom, M. E., Linden, R. M. & Parrish, C. R. (Eds.). Parvoviruses, Hodder Arnold Publication, 343-350

Phan, T. G., Vo, N. P., Bonkoungou, I. J. O., Kapoor, A., Barro, N., O'Ryan, M., Kapusinszky, B., Wang, C.& Delwart, E. (2012). Acute diarrhea in West African children: diverse enteric viruses and a novel parvovirus genus. *Journal of Virology* 86, 11024–11030.

Phan T.G., Sdiri-Loulizi K., Auoni M., Ambert-Balay K., Pothier P., Deng X. & Delwart E., 2014: New parvovirus in child with unexplained diarrhea, Tunisia, *Emerging Infectious Diseases* 20, 1911-1913

Phan, T. G., Dreno, B., Charlys, A., Li, L., Orlandi, P., Deng, X., Kapusinszky, B., Siqueira, J., Knol A. C., Halary, F., Dantal J., Alexander, K. A. Pesavento, P. A. & Delwart, E. (2016). A new protoparvovirus in human fecal samples and cutaneous T cell lymphomas (*mycosis fungoides*). *Virology* 496, 299–305.

Qiu, J., Söderlund-Venermo, M., & Young, N. S. (2017). Human parvoviruses. *Clinical Microbiology Reviews* 30, 43–113.

Rangarajan, S., Walsh, L., Lester, W., Perry, D.,Madan B., Laffan M., Yu, H., Vettermann, C., Pierce, G., F., Wong, W. Y. & Pasi J. (2017). AAV5–Factor VIII gene transfer in severe hemophilia a. *New England Journal of Medicine* 377, 2519–2530.

Riipinen, A., Väisänen, E., Lahtinen, A., Karikoski, R., Nuutila, M., Surcel, H. M., Taskinen H., Hedman K. & Söderlund-Venermo, M. (2010). Absence of human bocavirus from deceased fetuses and their mothers. *Journal of Clinical Virology* 47, 186–188.

Ruiz-Masó J. A., Machón, C., Bordanaba-Ruiseco, L., Espinosa, M., Coll, M. & Del Solar, G. (2015). Plasmid rolling-circle replication. *Microbiology Spectrum* 3, 1–23.

Sharp, C. P.,Vermeulen M., Nebie Y., Djoko, C. F., Tamoufe, U., Rimoin, A.W., Kayembe, P. K., Carr, J.K. Servant-Delmas, A., Laperche S., Harrison, A., Pybus, O. G., Delwart, E., Wolfe N. D., Saville, A.,Lefrere J.J. & Simmonds, P. (2010). Epidemiology of human parvovirus 4 infection in Sub-Saharan Africa, *Ermerging Infectious Diseases* 16, 1605-1607

Smits, S. L., Schapendonk, C. M. E., Beek, J. Van, Vennema, H., Schürch, A. C., Schipper, D.,Bodewes, R., Haagmans, B. L., Osterhaus, A. D. M. E. & Koopmans, M. P. (2014). New viruses in the Netherlands. *Emerging Infectious Diseases* 20, 1218–1222.

Storch, G. A. (2007). Diagnostic virology. In: Knipe, D. M. & Howley, P. M. (Eds.) Field's virology, vol 1, Lippincot, Williams & Wilkins, 565-604

Söderlund-Venermo, M., Lahtinen, A., Jartti, T., Hedman, L., Kemppainen, K., Lehtinen, P., Allander, T., Ruuskanen, O. & Hedman, K. (2009). Clinical assessment and improved diagnosis of bocavirus-induced wheezing in children, Finland. *Emerging Infectious Diseases* 15, 1423–1430.

Tang, P., & Chiu, C. (2010). Metagenomics for the discovery of novel human viruses, *Future Microbiology* 5,177–189.

Van der Meijden, E., Janssens, R. W. A., Lauber, C., Bouwes Bavinck, J. N., Gorbalenya, A. E. & Feltkamp, M. C. W. (2010). Discovery of a new human polyomavirus associated with trichodysplasia spinulosa in an immunocompromized patient, *PLOS Pathogens* 6, 1–10.

Väisänen, E., Fu, Y., Hedman, K., & Söderlund-Venermo, M. (2017). Human protoparvoviruses. *Viruses* 354

Väisänen, E., Kuisma, I., Phan, T. G., Delwart, E., Lappalainen, M., Tarkka, E., Hedman, K. & Söderlund-Venermo, M. (2014a). Bufavirus in feces of patients with gastroenteritis, Finland. *Emerging Infectious Diseases* 20, 1077–1079.

Väisänen, E., Paloniemi, M., Kuisma, I., Lithovius, V., Kumar, A., Franssila, R., Ahmed, K., Delwart, E., Vesikari, T., Hedman, K. & Söderlund-Venermo, M. (2016). Epidemiology of two human protoparvoviruses, bufavirus and tusavirus. *Scientific Reports* 6, 39267.

Väisänen, E., Mohanraj, U., Kinnunen, P. M., Jokelainen, P., Al-hello, H., Barakat, A. M.,Sadeghi, M., Jalililan, F. A., Majlesi, A., Masika, M., Mwaengo, D., Anzala, O., Delwart, E., Vapahlahti, O., Hedman, K. & Söderlund-venermo, M. (2018). Global distribution of human protoparvoviruses, *Emergin Infectious* Diseases 24, 1292-1299.

Väisänen, E., Fu, Y., Koskenmies, S., Fyhrquist, N., Wang, Y., Keinonen, A., Mäkisalo, H., Väkevä, L., Pitkänen, S., Ranki, A., Hedman, K. & Söderlund-Venermo, M. (2018). Cutavirus DNA in malignant and nonmalignant skin of cutaneous t-cell lymphoma and organ transplant patients but not of healthy adults, *Clinical Infectious Diseases* 20, ciy806

Vihinen-Ranta, M., Wang, D., Weichert, W. S., & Parrish, C. R. (2002). The VP1 N-terminal sequence of canine parvovirus affects nuclear transport of capsids and efficient cell infection. *Journal of Virology* 76, 1884-1891.

Vihinen-Ranta, M. & Parrish, C. (2006). Cell infection processes of autonomous parvoviruses. In: Kerr, T., Cotmore, S. F., Bloom, M. E., Linden, R. M. & Parrish, C. R. (Eds.). Parvoviruses, Hodder Arnold Publication, 157-163

Wang, N., Zhang, Y., Lei, X., Yu, W., Zhan, Y., Wang, D., Zhang, J., Wang, A., Xiao, L., Jiang, P. &Yang, Y. (2017). Optimized conditions for preserving stability and integrity of porcine circovirus type2 virus-like particles during long-term storage. *Journal of Virological Methods* 243, 146–150.

Wreghitt, T. G., & Sillis, M. (1985). A μ-capture ELISA for detecting *Mycoplasma pneumoniae* IgM: comparison with indirect immunofluorescence and indirect ELISA. *Journal of Hygiene* 94, 217–227.

Yahiro, T., Wangchuk, S., Tshering, K., Bandhari, P., Zangmo, S., Dorji, T., Tshering, K., Matsumoto, T., Nishizono, A., Söderlund-Venermo, M. & Ahmed, K. (2014). Novel human bufavirus genotype 3 in children with severe diarrhea, Bhutan. *Emerging Infectious Diseases* 20, 1037–1039.

Zadori Z., Szelei J., Lacoste M-C., Li Y., Garie S., Raymond P., Allaire M., Nabi I. R. and Tijssen P. (2001). A viral phospholipase A2 is required for parvovirus infectivity. *Developmental Cell* 1, 291–302

Zheng, L., Yuan, X., Xie, Z., Jin, Y., Gao, H., Song, J.,Zhang, R. F., Xu, Z. Q., Hou Y. D. & Duan, Z. (2010). Human bocavirus infection in young children with acute respiratory tract infection in, Lanzhou, China, *Journal of Medical Virology* 82, 282–288.

Zou, W., Wang, Z., Xiong, M., Chen, A. Y., Xu, P., Ganaie, S. S.,Badawi, Y., Kleiboeker, S., Nishimune, N.& Qiu, J. (2017). Human parvovirus B19 utilizes cellular dna replication machinery for viral DNA replication. *Journal of Virology* 92, e01881-17.

7.1.Internet resources

FIMM, Full service sequencing, https://www.fimm.fi/en/services/technology-centre/sequencing/capillary-sequencing-services/full-service-sequencing, visited 8.6.2018

HUS, Kliinisen mikrobiologian tutkimukset, http://www.hus.fi/hustietoa/sairaanhoitoalueet/hyks/huslab/laboratorion-erikoisalat/kliininen-mikrobiologia/Sivut/Kliinisen-mikrobiologian-tutkimukset.aspx. visited 8.11.2018

International Committee on Taxonomy of Viruses, ICTV, ssDNA Viruses, Parvoviridae, Genus: Protoparvovirus, https://talk.ictvonline.org/ictv-reports/ictv_online_report/ssdna-viruses/w/parvoviridae/1045/genus-protoparvovirus, visited 15.1.2019